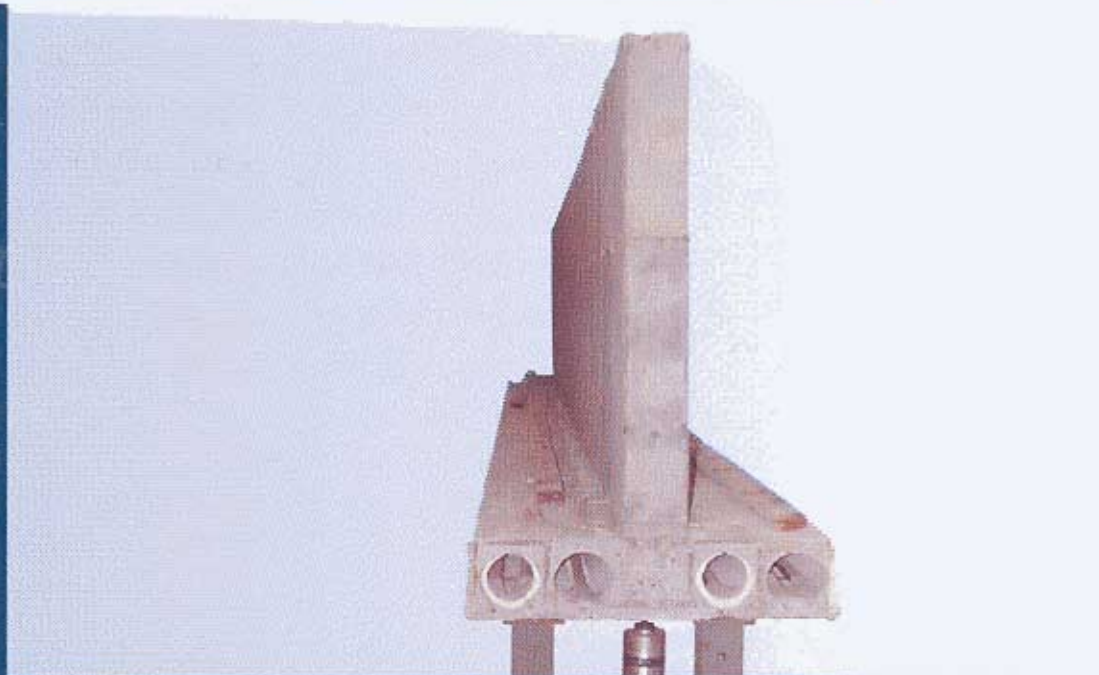




**HETEK**

Control of Early Age Cracking in Concrete  
Phase 7: Measured and Predicted  
Deformations in Hardening Concrete



Report No.106  
1997



Road Directorate Denmark  
Ministry of Transport

# IRRD Information

Title in English	HETEK -Control of Early Age Cracking in concrete - Phase 7:Measured and Predicted Deformations in Hardening Concrete	
Title in Danish	HETEK - Styling af revner i ung beton - Fase 7: Målte og beregnede deformationer i hærdnende beton	
Authors	Erik Steen Pedersen, Helle Spange	
Subject classification	Field 32	Concrete
Key words	Concrete	4755
	Creep	4732
	Cracking	5211
	Curvature	2870
	Deformation	5595
	Full scale	6227
	Test	6255
	Modulus of Elasticity	5919
	Heat	6743
	Development	9013
	Material (constr)	4555
	Measurement	6136
	Numerical	6432
	Properties	5925
	Shrinkage	4743
	Simulation	9103
	Stress Analysis	5573
	Thermal analysis	7152
	Stress (material)	5575
	Tension	5502
	Strength (mater)	5544
	Coefficient	5504
	Expansion	6720
	Research Project	8557
	Denmark	8028
Abstract	This report forms a part of the Danish Road Directorate's research programme called High Performance Concrete - The Contractor's Technology (abbreviated to HETEK). The report describes a full-scale test performed to demonstrate that stresses can be calculated in hardening concrete structures.	
UDK	691.32	
ISSN	09094288	
ISBN	87 7491 819 2	

# List of Contents

<b>0. Preface</b>	1
<b>1. Background</b>	3
<b>2. Aims</b>	4
<b>3. Experimental strategy</b>	5
<b>4. Experimental set-up</b>	6
4.1 Base slab	6
4.1.1 Geometry and reinforcement	6
4.1.2 Heating the base slab	6
4.1.3 Material properties	8
4.2 The wall	8
4.2.1 Geometry and reinforcement	8
4.2.2 Form	8
4.2.3 Material properties	8
4.3 Supports	9
4.4 Temperature measurements	9
4.5 Deformation measurements	10
4.6 Crack observations	12
<b>5. Carrying out the tests</b>	13
5.1 Casting	14
5.2 Curing conditions	14
5.3 Measurements	15
<b>6. Test results</b>	16
6.1 Test results	16
6.2 Evaluation of test results	17
6.2.1 Temperature measurements	17
6.2.2 Deformation measurements	18
6.2.3 Crack observations	22
<b>7. Comparison with calculations</b>	23
7.1 Temperature calculations	23
7.2 Stress calculations	24
<b>8. Conclusion</b>	30
<b>9. Literature</b>	31

# Appendices

- A Geometry and reinforcement
- B Determining the rigidity of the base slab
- C Measuring the coefficient of thermal expansion
- D Concrete properties
- E Placing of thermo-sensors
- F Measured and calculated concrete temperatures
- G Measured air temperatures
- H Measured temperatures in the hollow cores of the base slab
- I Measured deformations relative to the measuring bridge
- J Measured deformations relative to the fixed plane
- K Measured longitudinal deformations
- L Measured acoustic emission
- M Assumptions underlying the calculations

# 0. Preface

This project on control of early-age cracking is part of the Danish Road Directorate's research programme, High Performance Concrete - The Contractor's Technology <sup>1</sup>, abbreviated to HETEK (an acronym of Højkvalitetsbeton - Entreprenørens Teknologi).

In this programme, high performance concrete is defined as concrete with a service life in excess of 100 years in an aggressive environment.

The research programme includes investigations concerning the contractor's design of high performance concrete and execution of the concrete work with reference to the required service life of 100 years.

The HETEK research programme is divided into segments with the following topics:

- chloride penetration
- frost resistance
- control of early-age cracking
- compaction
- curing (evaporation protection)
- trial casting
- repair of defects

The Danish Road Directorate invited tenders for this research programme which is mainly financed by the Danish Ministry for Commerce and Industry - The Commission of Research and Development Contracts.

The present report refers to the segment of the HETEK project which deals with the control of early-age cracking.

For durability reasons reinforced structural members should be well protected against penetration of water, chloride, etc. This means that cracks should be avoided or at least the crack-width limited. Cracks can form during the hardening process. An evaluation of the risk of crack formation involves a stress analysis. In stress analysis of hardening concrete structures, the load consists of the differences in thermal strains that arise from the heat of hydration. The mechanical properties (including autogenous shrinkage) of the concrete also change during the hardening process. If a stress analysis shows high stresses compared to the tensile strength there is a high risk of crack formation.

The purpose of this project is to investigate these effects and to prepare guidelines for the control of early-age cracking.

The project was carried out by a consortium consisting of:

The Danish Concrete Institute, represented by:

Højgaard & Schultz A/S  
Monberg & Thorsen A/S  
RAMBØLL  
COWI

and

The Danish Technological Institute, represented by the Concrete Centre

and

The Technical University of Denmark, represented by the Department of Structural Engineering and Materials.

Two external consultants, Prof. Per Freiesleben Hansen and manager Jens Frandsen, are connected with the consortium.

The present report, "Measured and Predicted Deformations in Hardening Concrete", was prepared by the Danish Technological Institute - Concrete Centre.

# 1. Background

Traditionally, crack formation is to be avoided for reasons of durability, serviceability and aesthetics. Cracks form as a result of differences in temperature and shrinkage movements between structural components and between the interior and surface of a structural component. In hardening concrete structures the situation is complicated by the heat developed in the concrete and the changes in material properties arising from the hardening process.

For prismatic structures (e.g. a wall on a base slab), 3-dimensional analyses show that the stress distribution does not change from cross-section to cross-section in the region between the end-zones. As the normal stress at the end cross-section is zero, the normal stresses in the intermediate zone are converted to shear stresses at the end-zones (Figure 1.1).

In the intermediate zone, where there are no shear deformations, it can therefore be assumed that plane sections remain plane. The distribution of normal stresses in the cross-section can be determined by a non-stationary cross-section calculation. The calculation includes autogenous deformations from temperature and shrinkage differences and from changes in material properties, cf. "Control of Early Age Cracking in Concrete - Guidelines" [Pedersen et al., 1997]. This method is used in several commercial computer programmes.

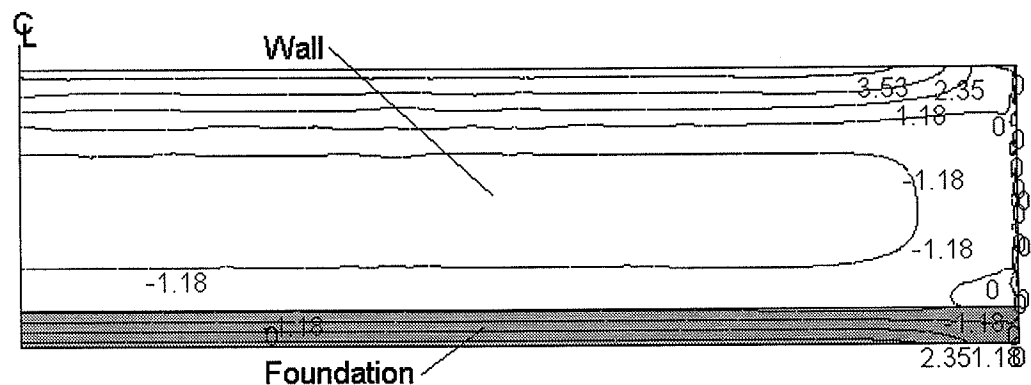


Figure 1.1. Isoquants for the longitudinal stress component,  $\sigma_z$

## 2. Aims

The purpose of the present project segment is to demonstrate that the "hardening-stress theory" described in Section 1 can be used for typical structures.

The assumption that plane sections remain plane implies that the curvature along a structural component will be constant. However, this does not apply to the end-zones due to shear deformations. The test is intended to show that the curvature is constant when the distance to the end-face exceeds a certain value.

The test is also intended to give a set of measurements that can be compared with the theoretical values.



### 3. Experimental strategy

The test was carried out under laboratory conditions on a 10 m long wall on a base slab. The cross-section is shown in Figure 3.1.

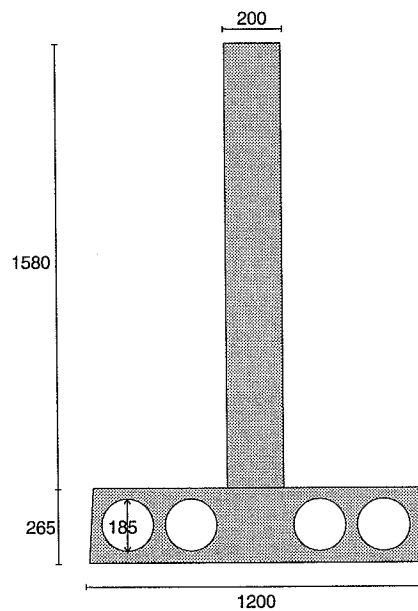


Figure 3.1. Dimensions of the cross-section

The dimensions were chosen so that the structure could be handled in the laboratory. For the same reason a prefabricated hollow-core floor unit was chosen as the base slab. Procedures described in the following ensured that the temperature and stress histories in the wall correspond to those that arise in actual structures.

As the wall is relatively thin, the temperature will not be as high as in a "real" structure. To obtain a realistic temperature history the wall was highly insulated.

The chosen base slab is relatively flexible, so that casting the wall on the slab presented less of a problem than in a "real" structure. To compensate for the low axial rigidity the slab was heated and the wall simultaneously cooled. The base slab thus expanded while the wall contracted, resulting in increased tensile stresses in the wall. The heating was adjusted in order to obtain a realistic stress history in the wall.

The structure was simply supported to eliminate the uncertainty concerning interaction with a sub-base. This topic is dealt with in another part of the project [Andersen, 1997].

# 4. Experimental set-up

## 4.1 Base slab

### 4.1.1 Geometry and reinforcement

The base slab is a standard floor unit with 5 hollow cores, 1200 mm wide, 265 mm thick and 10 m long. The central core was filled with concrete and stirrups placed in it at the factory. The slab was prestressed with 10 1/2" lines at the bottom and 4 1/2" lines at the top to avoid unintentional crack formation. All lines stressed to an effective elongation of 6‰. The geometry and reinforcement of the base slab are shown in Figure 4.1 and Appendix A.

### 4.1.2 Heating the base slab

One heating element is placed in each of the two inner cores and two in each of the outer cores as shown in Figure 4.2. The elements have a power of 14 W/m. To avoid failure of elements as a result of overheating, they are placed in UNP30 steel profiles and surrounded with mortar. To distribute the heat to the entire cross-section, air is circulated in the cores. This is done by a ventilator in each core, placed in such a way that there are two ventilators at each end of the slab. The air speed was measured at the centre of one core and found to be approx. 1.5 m/s. An insulated chamber was built around each end of the slab so that air could circulate without mixing with the colder air of the laboratory. These measures are shown in Figures 4.3 - 4.5.

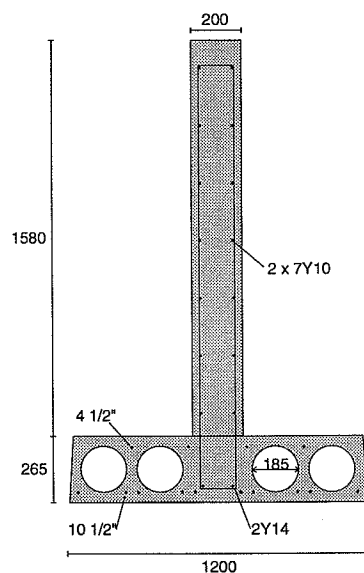


Figure 4.1. Geometry and reinforcement

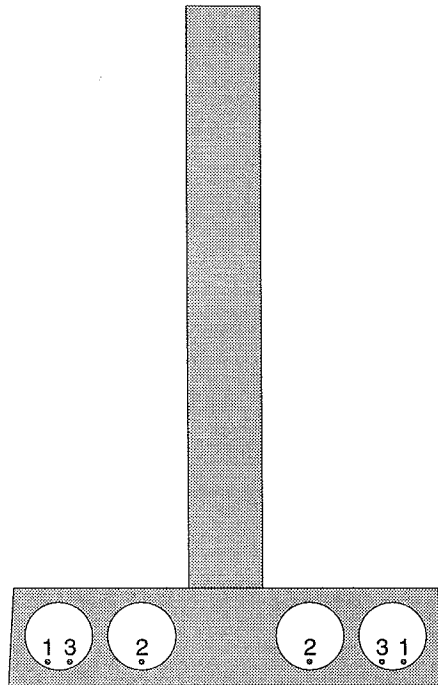


Figure 4.2. Numbering of heating elements in the base slab.

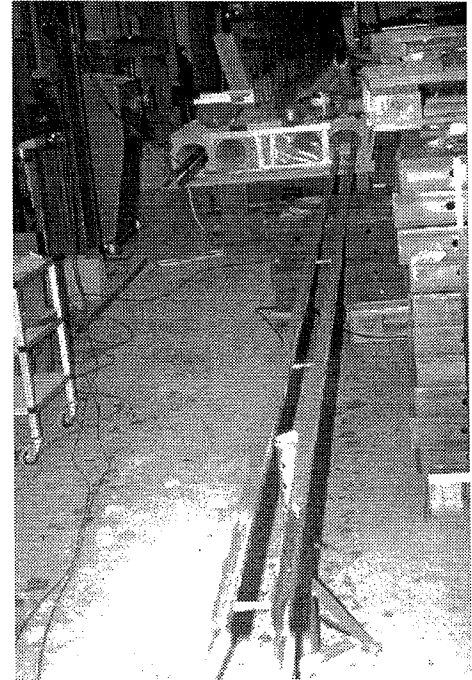


Figure 4.3. The heating elements are cast in UNP30 profiles before placing in the hollow cores. It can be seen that the inner cores are temporarily covered with plastic.

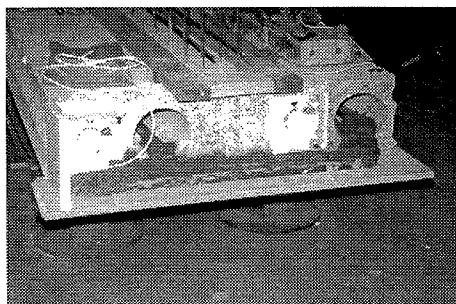


Figure 4.4. Placing of ventilators at one end of the slab. At the opposite end the ventilators are placed in the other two cores.

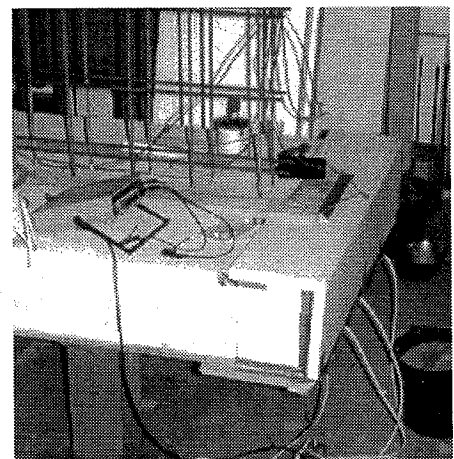


Figure 4.5. An insulated chamber is built around each end of the slab to prevent the air circulating in the cores from mixing with laboratory air.

### **4.1.3 Material properties**

The modulus of elasticity of the base slab was determined by a loading test carried out 4 days before casting the wall, and was found to be 45000 MPa.

The age of the base slab was then 57 days. During the test the form was placed on the slab, but not fixed to it. This corresponds to the situation during the test after the setting time of the wall. The determination of the rigidity is described in Appendix B.

The coefficient of thermal expansion of the base slab  $\alpha$  was found to be  $1.01 \cdot 10^{-5} \text{C}^{-1}$ . The determination was made on a test specimen cut out of the slab after the conclusion of the test. The determination is described in Appendix C.

## **4.2 The wall**

### **4.2.1 Geometry and reinforcement**

The wall is 200 mm thick, 1580 mm high and 10 m long. It is reinforced with vertical and horizontal bars. The vertical reinforcement consists of Ks550 Y10 stirrups placed at 200 mm intervals. The stirrups are 140 mm wide and 1695 mm high, and cast into the slab at the factory. The horizontal reinforcement consists of 7 Ks550 Y10 on each side, uniformly distributed over the height of the wall. The geometry and reinforcement arrangement are shown in Figure 4.1 and Appendix A.

### **4.2.2 Form**

The wall was cast in a form built up of standard cassettes consisting of steel frames of 5 x 90 mm rectangular profiles covered with 15 mm plywood. The two sides of the form were connected by anchor bars placed at the top of each cassette. The building of the form is shown in Figure 4.6. During casting, the form was fixed to a foot-strip, screwed to the base slab. In addition, the form was supported by two diagonal struts that were removed immediately after casting. After the setting time of the wall, the form was released from the foot-strip and anchor bars. The form was kept during the entire test period. The total height of the form including the foot-strip was 1.84 m, i.e. higher than the completed wall.

### **4.2.3 Material properties**

The wall was cast with concrete No. 6021 supplied by 4K-BETON. The mix is given in Appendix D, which also gives the properties of the concrete determined by tests. Slump, air content and density were determined on delivery; the results are shown in Appendix D.

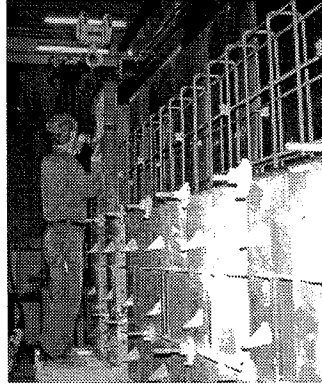


*Figure 4.6. Building the form.*

### **4.3 Supports**

The 10 m long structure is simply supported with a span of 8 m and a 1 m cantilever at each end. The slab is supported at one end by two ball-races on each side. The ball-races are placed under the ribs between the cores. At the opposite end the slab is supported at the centre by a ball-race mounted on a roller-bearing.

For safety reasons the structure was temporarily supported at two points at each end during casting. After casting it was placed on permanent supports with the aid of a hydraulic jack.

### **4.4 Temperature measurements**

The temperature of the concrete was measured by thermo-sensors placed in the wall and base slab as shown in Figure 4.7 and Appendix E. The thermo-sensors in the wall were mounted prior to casting. The thermo-sensors in the slab were bored in. The bore-holes were then filled with cotton waste and plastic padding. The air temperature was measured at the central cross-section under the base slab, at the top of the wall and the bottom of the wall (Figure 4.7). In addition the air temperature was measured in two of the base slab cores, about 0.2 m from the end-face. All temperatures were recorded at 10-minute intervals by a datalogger.

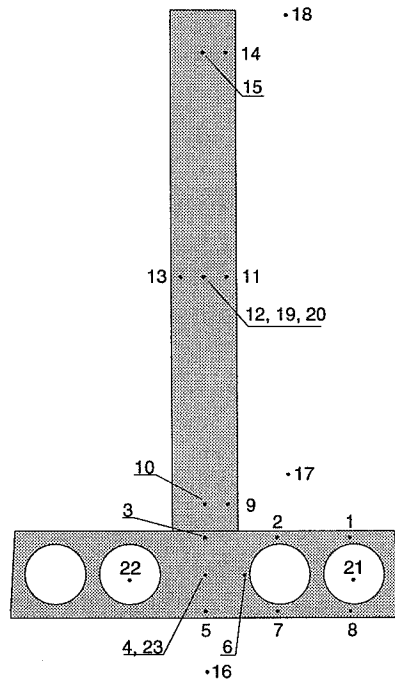


Figure 4.7. Positions of thermo-sensors. Sensors 1-18 are at the central cross-section. Sensor 19 is 1 m from the central section. Sensor 20 is 2 m from one end. Sensor 23 is 2.4 m from the central section. See Appendix E.

## 4.5 Deformation measurements

The deformations of the structure are measured by means of electronic transducers. The measurements are recorded at 10-minute intervals by a datalogger.

The deflection figure is measured in relation to a 4.20 m long measuring bridge suspended under the base slab by threaded rods. Measurements are made at 6 points, equidistant on the beam axis as shown in Figure 4.8. The transducers are mounted on pins fixed to the concrete by angle plates and locked into holes in the measuring bridge (see Figure 4.11).

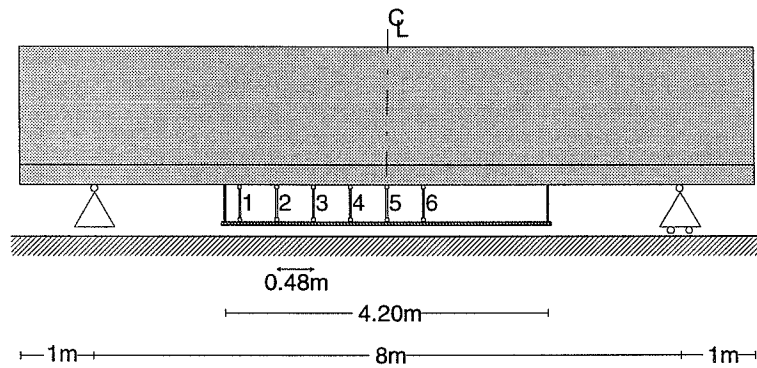


Figure 4.8. Sketch showing positions of vertical movement-transducers for determining the deflection figure.

The total deflection is measured at the central cross-section, at one end of the structure and at 1.55 m from the end, as shown in Figure 4.9. The deflections are measured relative to the plane on which the transducers are fixed. The transducers measure up to the underside of the base slab, but are not fixed to it.

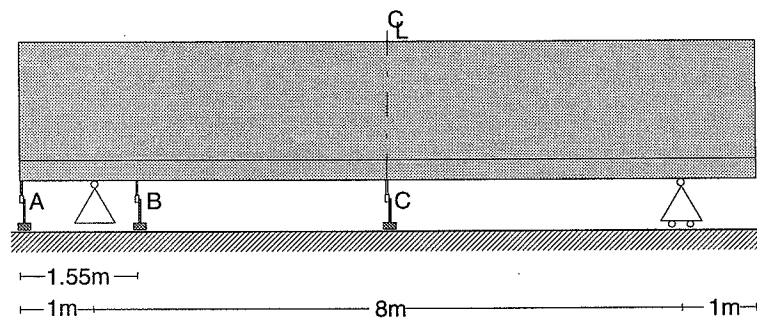


Figure 4.9. Sketch showing positions of movement-transducers for determining the total deflection.

Longitudinal deformations are measured at the central cross-section and at 0.5 m from that section. At both positions transducers are placed at the top of the wall and the over- and undersides of the base slab as shown in Figure 4.10. The measurements are made over a length of 1 m. The transducers are mounted on the base slab by means of bored-in pins. The transducers at the top of the wall are placed in connection with the casting in such a way that the pins are cast in. The transducers at the top of the wall are locked until the wall has set.

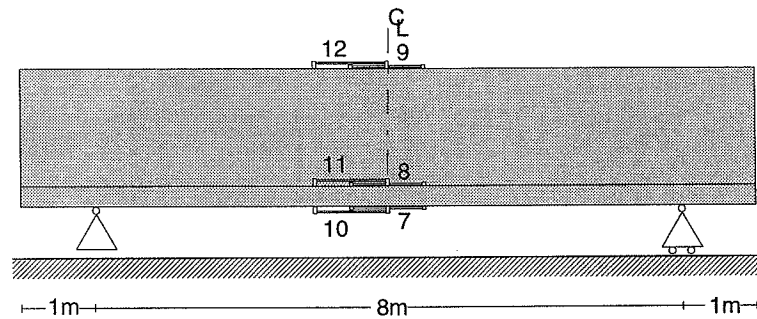


Figure 4.10. Sketch showing positions of movement-transducers for determining horizontal deformations. The measurements are made over a length of 1 m.

## 4.6 Crack observations

To detect the moment at which cracks form, the acoustic emission is measured. A microphone is placed on the top of the base slab about 0.22 m from the wall and 1 m from the central cross-section.

After the conclusion of the test, the form is removed and the positions and sizes of the cracks are measured.

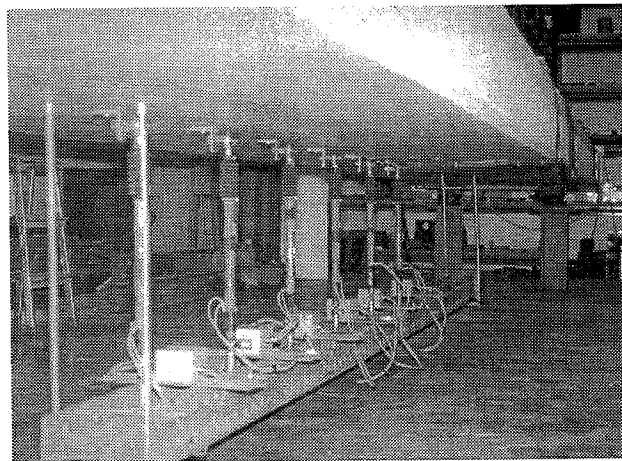


Figure 4.11. Mounting of vertical transducers for determining the deflection figure. The measurements are made in relation to a measuring bridge suspended from the base slab by threaded rods.

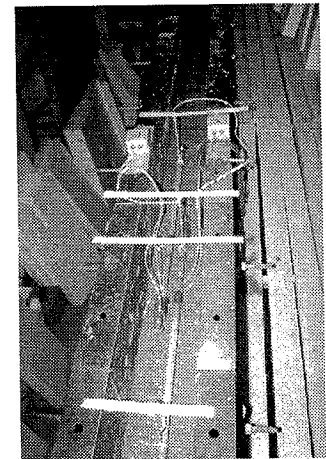


Figure 4.12. Mounting of horizontal transducers in the top of the wall immediately after casting.



## 5. Carrying out the tests

The tests were carried out in the period 16.12.1996 to 2.1.1997. An overview of the procedure is shown in Table 5.1. It is described in detail in the following Sections.

Age [hours]	Activity
0	Mixing time. Concrete temperature 22 °C
0.8	Concrete delivered. Concrete temperature 19.5 °C
1.0 - 2.2	Casting of wall
2.7	Covering of wall-top with plastic and insulation
3.1	Lowering onto permanent supports
3.5	Vertical deformation measurements begin
9.5-9.6	Longitudinal transducers released
9.7	Longitudinal deformation measurements begin
9.7-9.9	The form is released
9.9-11.2	Insulation of the wall
11.6	The top is covered with plastic
22.4	Heating element No.1 activated
22.6-23.1	Insulation of topside of base slab
47.4	Heating element No. 2 activated
98.3	Acoustic emission measurement begins
99.7-100.1	Insulation is removed from wall sides
117.7	Heating element No. 3 activated
405	Test concluded

Table 5.1. Overview of test procedure. Time = 0 corresponds to the mixing time - 1996-12-16, 12:16 hrs. The underside and sides of the base slab were insulated prior to the test.

## 5.1 Casting

The base slab was 61 days old when the wall was cast. It was in the laboratory for 60 days of this time.

To ensure that adhesion between wall and base slab corresponded to that in a real structure, the construction joint was cleaned by brushing. The joint was moistened about 4 hours before casting.

The concrete was transported from 4K-BETON, Islands Brygge, to DTI Taastrup in a mobile drum. The temperature of the concrete was 22°C during mixing and 19.5°C on arrival 0.8 hours after mixing.

Casting of the wall began one hour after mixing and lasted 1.2 hours. After casting the diagonal struts were loosened and the structure lowered onto its permanent supports.

The form was released about 10 hours after mixing. The compressive strength at that time was found to be 0.6 MPa.

## 5.2 Curing conditions

Before casting the wall, the base slab was insulated with polystyrene on the sides and bottom as shown in Figure 5.1. The insulation was glued onto the concrete. The insulation was placed as close as possible to the movement transducers.

Immediately after casting, the top of the wall was covered with plastic and insulated with 100 mm polystyrene panels. The plastic and insulation were placed between the sides of the form (see Fig. 5.1). The insulation was placed above the horizontal movement transducers.

Immediately after releasing the form, the wall was insulated with 100 mm polystyrene panels. The insulation was placed outside the form. Because of the shape of the anchor rods, there was a space between insulation and form. To reduce air circulation, a plastic cover was placed on the top (Fig. 5.1).

About 22 hours after mixing, heating element No. 1 was activated. The top of the base slab was simultaneously insulated (Fig. 5.1). The insulation was placed as close as possible to the horizontal movement transducers. Insulation was also placed on these. About 47 hours after mixing, heating element No. 2 was activated.

The insulation and plastic cover on the wall were removed about 100 hours after mixing. The insulation on the top of the wall was retained throughout the test period.

About 118 hours after mixing, heating element No. 3 was activated.

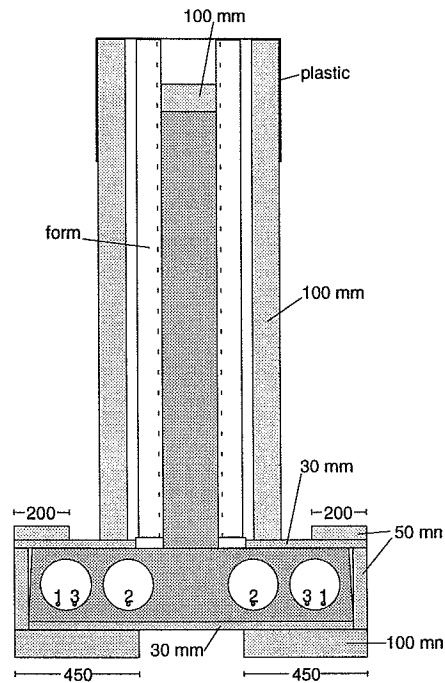


Figure 5.1. Insulation and heating elements.

### 5.3 Measurements

Temperature measurements began at the time of casting.

Measurements of deformation relative to the measuring bridge and the fixed plane were started immediately after the structure had been placed on the permanent supports, i.e. 3.5 hours after mixing.

The measurements of horizontal deformation were started immediately before loosening the form, i.e. about 10 hours after mixing.

Measurement of acoustic emission began about 98 hours after mixing.

At the end of the test the form was removed and inspection for cracks carried out.

# 6. Test results

## 6.1 Test results

All the measurements are given in Appendices F-L. The results consist of:

- concrete temperatures Appendix F
- air temperatures Appendix G
- temperatures in the holes of the base slab Appendix H
- vertical deformations relative to measuring bridge  
(transducer Nos. 1-6, Fig. 4.8) Appendix I
- vertical deformations relative to fixed plane  
(transducer Nos. A-C, Fig. 4.9) Appendix J
- horizontal deformations  
(transducer Nos. 7-12, Fig. 4.10) Appendix K
- acoustic emission Appendix L

The measured properties of the fresh concrete are given in Appendix D.

All results are shown as a function of time. In the diagrams,  $t = 0$  corresponds to the time of mixing except for the measurement of acoustic emission, where  $t = 0$  corresponds to 98.3 hours after mixing.

A positive deformation means that the structure moves upwards or expands longitudinally at the point in question.

Appendices I and K show both the measured and the temperature-adjusted deformations.

The vertical deformations relative to the measuring bridge are compensated for temperature movements in the transducers as well as in the measuring bridge. The compensation for the temperature movements of the transducers is based on temperature changes measured by means of built-in temperature sensors. The temperature sensitivity of the transducers varies between  $0.69 \cdot 10^{-5}$  and  $0.75 \cdot 10^{-5} \text{ m}/^\circ\text{C}$ . As the compensation for the temperature movements of the measuring bridge is the same for all six transducers, it only influences the absolute deflections relative to the measuring bridge. The compensation for the temperature movements of the measuring bridge does not influence the deflection figure or the curvature.

The horizontal deformations are compensated for temperature movements in the transducers based on temperature changes measured by means of built-in temperature sensors. The temperature sensitivity of the transducers varies between  $1.22 \cdot 10^{-5}$  and  $1.35 \cdot 10^{-5} \text{ m}/^\circ\text{C}$ .

The vertical deformations relative to the fixed plane shown in Appendix J are not compensated for temperature movements.

After removal of the form, a crack was observed about 0.2 m from the central section, where two form cassettes join. The crack was observed on both sides of the wall. The crack measurements are given in Table 6.1.

	Wall, east side	Wall, west side
Start of crack (measured from base slab) [m]	approx. 0.14	approx. 0.15
Crack length [m]	approx. 0.59	approx. 0.39
Crack width [mm]	approx. 0.05	approx. 0.1

Table 6.1. Observed crack 0.2 m from central section.

## 6.2 Evaluation of test results

### 6.2.1 Temperature measurements

Figure 6.1 shows the temperature measured at the centre of the wall and the centre of the foundation. All the temperature measurements are given in Appendices F-H.

It can be seen that the temperature in the wall reaches a max. of approx. 36°C when  $t =$  approx. 20 hours. The temperature at the centre section (No.12) and 1 m from the centre (No.19) are practically equal. The max. temperature 2 m from the end (No.20) can be seen to be 1°C lower. The wall had cooled after about 192 hours, i.e. long before the end of the test.

It can be seen that the temperature at the centre of the wall reaches a maximum of 33-34°C after approx. 192 hours. The difference between the measurement at the centre section (No. 4) and the section 2.4 m from it (No. 23) is probably due to the placing of a movement-transducer at the centre section, which made insulation difficult.

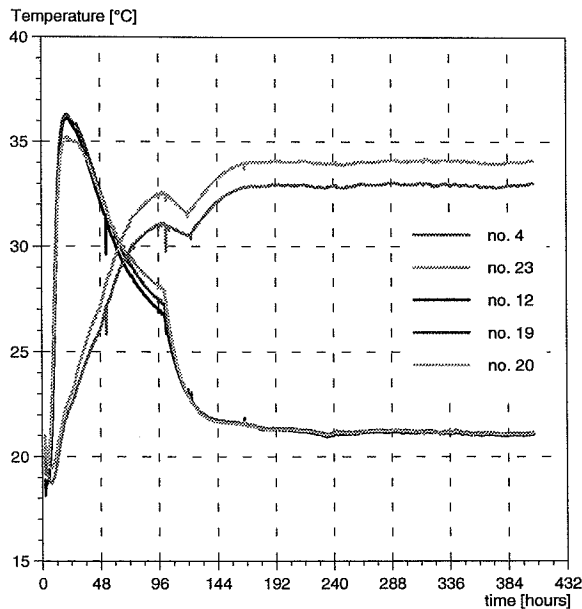


Figure 6.1. Measured temperatures at the centre of the foundation (Nos. 4 and 23) and the centre of the wall (Nos. 12, 19 and 20).  $t = 0$  at mixing. The placing of the thermo-sensors is shown in Figure 4.7.

### 6.2.2 Deformation measurements

Figure 6.2 shows the deformations relative to the measuring bridge as a function of time. The measurements began 3.5 hours after mixing. It can be seen that the structure bends upwards in the heating phase and downwards in the cooling phase. The deformations in transducers Nos. 4 and 6 must be equal for reasons of symmetry. The agreement between the measured values from these two transducers is an indicator of the accuracy of the measurements, which can be seen to be high.

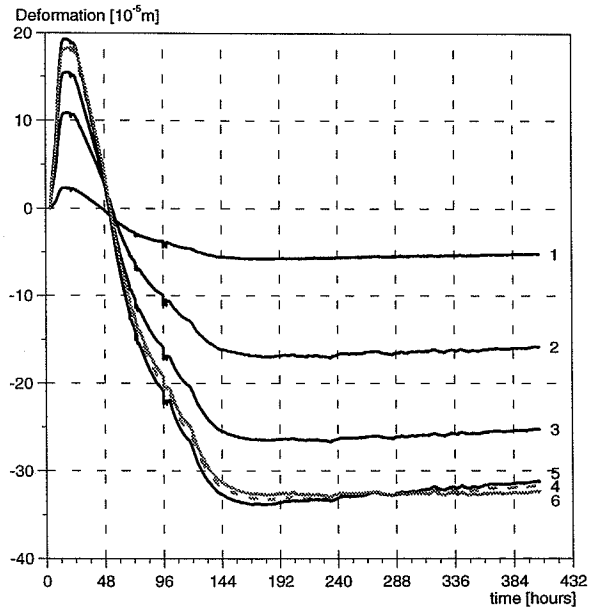


Figure 6.2: Deformations relative to the measuring bridge. The measurements are also given in Appendix I.  $t = 0$  at mixing.

In Figure 6.3 the deflection figures corresponding to a series of times are shown. If the curvature is constant along the structure, the deflection figure will be a segment of a circle. In Figure 6.3 circular curves have been drawn in, and they are in good agreement with the measured deflections except for the measurements at  $x = -1.96$  m (transducer No. 1, cf. Figure 4.8). It can thus be stated that the theoretical assumption of constant curvature is justified, at least for the central 3 m of the structure.

For  $t = 188.75$  and  $399.75$  hrs., circles cannot be drawn as the deflection of the transducer placed at the central section ( $x = 0$ ) is less than the deflections of the adjacent transducers. This is probably due to cracking in the wall.

Table 6.2 gives the radius of each of the circles shown in Figure 6.3. The corresponding curvature (the reciprocal of the radius) is also given.

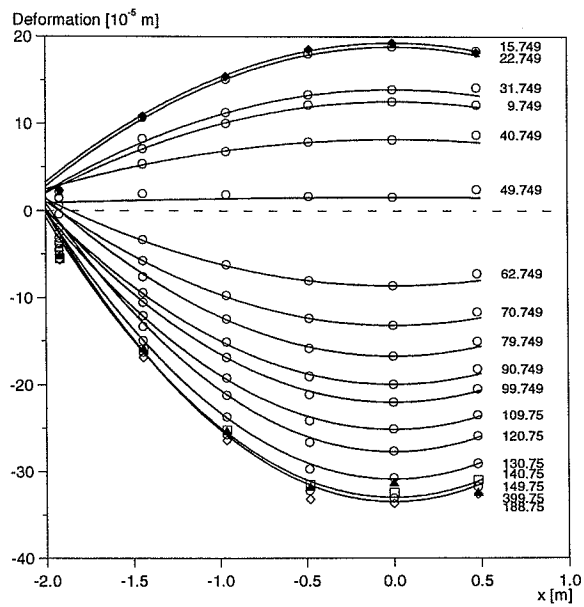


Figure 6.3. Deformations relative to the measuring bridge at various times. The deflection figures are segments of circles of which the radii are given in Table 6.2.  $x = 0$  corresponds to the central section.

Time	Radius [m]	Curvature [ $m^{-1}$ ]	Time	Radius [m]	Curvature [ $m^{-1}$ ]
3.50	-	0	90.75	$1.00 \cdot 10^4$	$-10.000 \cdot 10^{-5}$
9.75	$-1.90 \cdot 10^4$	$5.263 \cdot 10^{-5}$	99.75	$0.90 \cdot 10^4$	$-11.111 \cdot 10^{-5}$
15.75	$-1.25 \cdot 10^4$	$8.000 \cdot 10^{-5}$	109.75	$0.80 \cdot 10^4$	$-12.500 \cdot 10^{-5}$
22.75	$-1.25 \cdot 10^4$	$8.000 \cdot 10^{-5}$	120.75	$0.70 \cdot 10^4$	$-14.286 \cdot 10^{-5}$
31.75	$-1.70 \cdot 10^4$	$5.882 \cdot 10^{-5}$	130.75	$0.65 \cdot 10^4$	$-15.385 \cdot 10^{-5}$
40.75	$-3.50 \cdot 10^4$	$2.857 \cdot 10^{-5}$	140.75	$0.62 \cdot 10^4$	$-16.129 \cdot 10^{-5}$
49.75	$-30 \cdot 10^4$	$0.333 \cdot 10^{-5}$	149.75	$0.60 \cdot 10^4$	$-16.667 \cdot 10^{-5}$
62.75	$2.00 \cdot 10^4$	$-5.000 \cdot 10^{-5}$	188.75	-	-
70.75	$1.40 \cdot 10^4$	$-7.143 \cdot 10^{-5}$	399.75	-	-
79.75	$1.10 \cdot 10^4$	$-9.091 \cdot 10^{-5}$	-	-	-

Table 6.2. Curvatures based on measured deformations, cf. Figure 6.3. Curvature =  $1/\text{radius}$ .



The measured horizontal deformations are shown in Appendix K.

As mentioned in Section 6.1, temperature movements have been compensated on the basis of measurements with the built-in temperature-sensors. However, a difference was observed between the temperature changes recorded by this sensor and by an external thermo-sensor placed at one end of a transducer. The cause is probably the conduction of heat from the concrete to the transducers (and in the reverse direction) via the mounting pins. This means that the temperature movements of the transducers are evaluated erroneously. The temperature history cannot be expected to be the same for the transducers on the top of the wall, on the top of the base slab and at the bottom of the base slab; this is partly a result of different concrete temperatures, and partly of different degrees of insulation.

Measurements of the horizontal deformations therefore cannot be used to determine the curvature of the structure at the two sections. But a comparison of the measurements at the two sections can be made, as the error from temperature movements will be practically the same for transducers placed at the same height. It can be seen that there is good agreement between the measured deformations at the central section and at the section 0.5 m from it. This supports the conclusion that the curvature is constant in the central zone of the structure.

For the vertical movement-transducers, the error will be small; as mentioned in Section 4.5, these transducers are mounted indirectly on pins fixed to the concrete by angle profiles. Any small error in the estimation of temperature will result in practically the same error in the temperature movements for all six transducers, and thus have no effect on the deflection figures and curvatures.

Figure 6.4 shows the deflection of the centre of the structure relative to that of the end, based on measurements made in relation to the fixed plane. The missing temperature compensation is considered to be the same for both transducers and therefore has no effect on the deflection difference. The structure bends upwards with a maximum of approx. 1.2 mm in the heating phase and downwards with a maximum of approx. 1.9 mm in the cooling phase. The deformations are thus quite small.

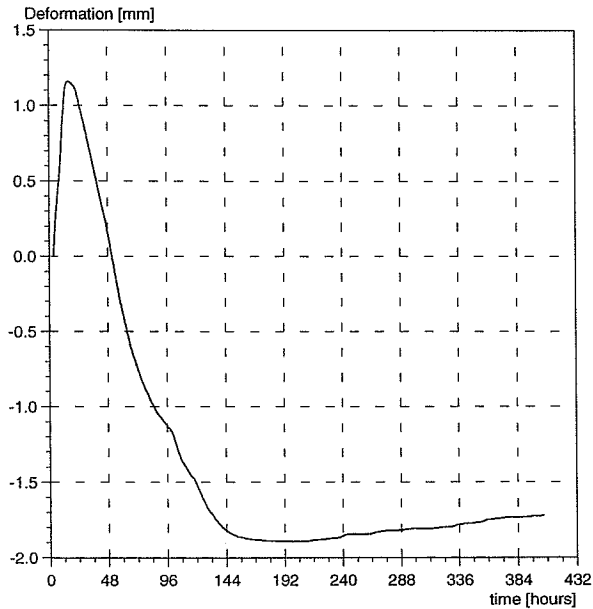


Figure 6.4. Deflection at the centre of the structure relative to the deflection at the end (total camber).

### 6.2.3 Crack observations

The measurements of acoustic emission were carried out in the period 98.3 to 152.5 hours after mixing and are given in Appendix L. The high values at the start are connected with testing the equipment. There is a tendency for the signal to increase in intensity in the period  $1.5 \cdot 10^5$  to  $1.7 \cdot 10^5$  seconds after the start of the measurements, corresponding to 140 - 145.5 hours after mixing. The microphone was placed 0.76 m from the crack and the increased signal may indicate that the crack formed in this period.

## 7. Comparison with calculations

A theoretical calculation of the test was carried out by means of the programme CIMS-2D [DTI Building Technology, 1995]. Due to symmetry only half of the cross-section was modelled.

### 7.1 Temperature calculations

In a stress calculation for a hardening structure, temperature functions as a load. To ensure that the correct loading is used in the calculation, it is important that the calculated temperatures agree with the measured.

Figure 7.1 shows a comparison of measured and calculated temperatures for the centre of the wall and the centre of the foundation. Comparisons for all measuring points are given in Appendix F. The input data used are given in Appendix M.

The casting temperature of the concrete was taken as 18 °C, corresponding to the temperature measured halfway through casting. The maturity of the concrete was then 1.5 hours. The calculation takes this into account by holding the temperature constant at 18 °C until a maturity of 1.5 hours has been attained. This means that 0.17 hours has been added to all times shown in Appendix M relative to the period elapsed since mixing.

The heat development of the concrete was measured, cf. Appendix D. In the calculation the measured heat development curve was used and not the curve determined by regression.

The air temperature used in the calculation is based on the temperature measured at the wall. The wind speed was taken to be 1 m/s.

The small dimensions of the structure combined with relatively thick insulation means that the energy needed to heat the insulation cannot be ignored. The insulation of the base slab is therefore included in the cross-section modelling (Appendix M). Due to the air column between form and insulation, satisfactory agreement cannot be obtained by following the same procedure for the wall insulation. It was therefore decided to use a variable transmittance, cf. Appendix M, in order to obtain good agreement (Figure 7.1 and Appendix F).

The heating of the base slab is modelled by giving the boundary of each hollow core a temperature history corresponding to the temperature measured in the core. A wind speed of 5 m/s was assumed in the cores, as this gives a better agreement between measured and calculated temperatures than the measured wind speed of 1.5 m/s. As mentioned above, it is important to obtain as good an agreement as possible in order to correctly predict the stress development.

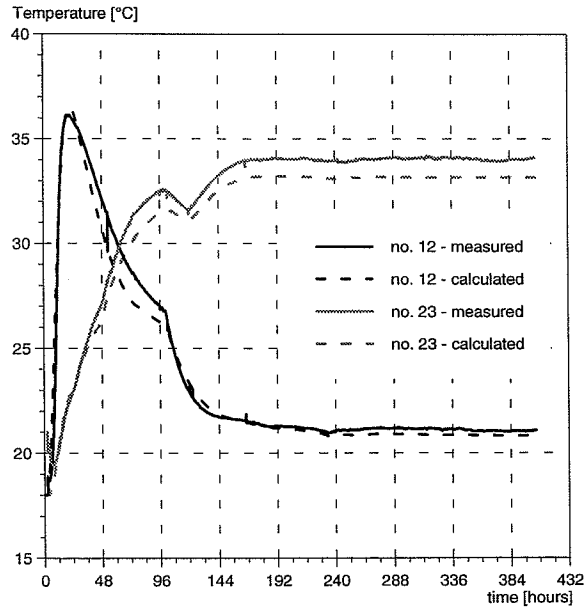


Figure 7.1. Comparison of measured and calculated temperatures at the centre of the wall (No. 12) and the centre of the base slab (No. 23). Comparisons for the other points can be found in Appendix F.

## 7.2 Stress calculations

A stress calculation can be carried out on the basis of the temperature calculation. This results in a determination of curvature as a function of time.

Figure 7.2 shows a comparison of the curvature based on measured deformations (cf. Table 6.2) and the calculated curvature as a function of time. The deviation between measured and calculated curvature can be seen to be approx.  $0.1 \cdot 10^{-4} \text{ m}^{-1}$  in the heating phase and approx.  $0.2 \cdot 10^{-4} \text{ m}^{-1}$  in the cooling phase.

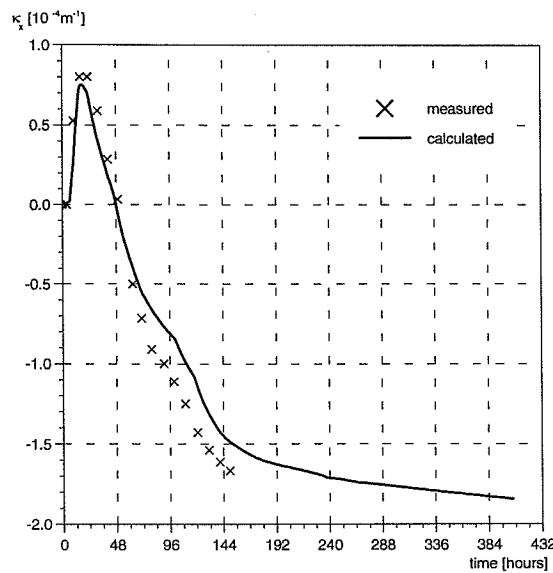


Figure 7.2. Comparison of measured and calculated curvature. The curvature is zeroed at the start of deformation measurings ( $t = 3.5$  hrs.).

Figure 7.3 shows the distribution of the normal stresses at  $t = 16$  hrs.. It can be seen that tensile stresses appear at the top of the wall and compressive stresses appear at the bottom. The maximum compressive stress can be seen to appear in a small distance above the construction joint. This is due to the cooling of the wall against the base slab.

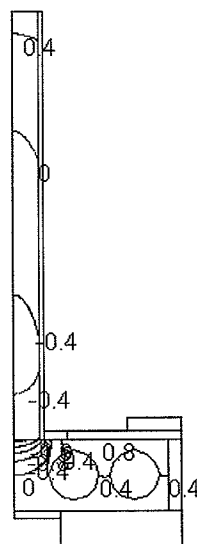


Figure 7.3. Distribution of normal stresses at  $t = 16$  hrs.. Due to symmetry only half of the cross-section was modelled.

Figure 7.4 shows the distribution of the normal stresses at  $t=144$  hrs.. At this time tensile stresses appear at the bottom of the wall and compressive stresses appear at the top.

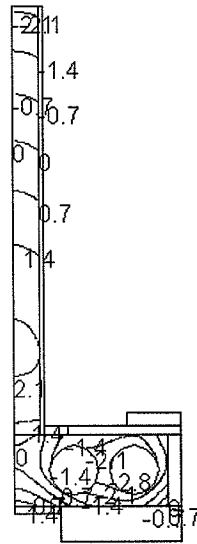


Figure 7.4. Distribution normal stresses at  $t= 144$  hrs.. Due to symmetry only half of the cross-section was modelled.

The calculation does not make it possible to determine the absolute deflection of the structure, as shear deformations in the end-zones are not taken into account.

The stress calculation corresponding to the curvature development can be used to determine the degree of utilization of tensile strength as a function of time. Figure 7.5 shows the development of the ratio between tensile stress and splitting tensile strength in two points. In these points the maximum utilizations are obtained. One point is placed in the corner at the top of the wall. The other point is placed in the center of the wall 0.32 m above the construction joint. At the moment of crack formation as determined by acoustic emission the degree of utilization is approx. 74%. In the heating phase a higher degree of utilization (approx. 89%) is seen. This indicates that cracks were formed at this very early age, too.

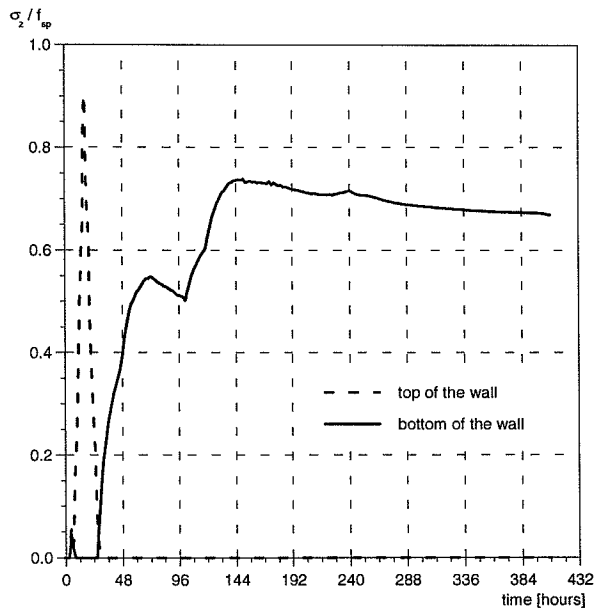


Figure 7.5. Ratio between tensile stress and splitting tensile strength in selected points. One point is placed in the corner at the top of the wall. The other point is placed in the center of the wall 0.32 m above the construction joint

Figure 7.6 shows the distribution of the utilization of the splitting tensile strength at  $t = 16$  hrs. It can be seen that the high degree of utilization occurs locally in the corner at the top of the wall. It was not possible to observe whether or not cracks appeared during the heating phase as the wall was insulated (cf. Figure 5.1). Such cracks would close during the cooling phase as compressive stresses are build up in the top of the wall (cf. Figure 7.3). The cracks could not be observed after stripping the insulation.

As the high degree of utilization occurs in a very small area, the curvature of the structure will not be affected worth mentioning.

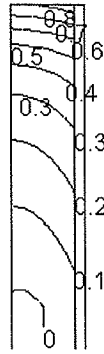


Figure 7.6. Distribution of the ratio between tensile stress and splitting tensile strength in the top of the wall at  $t = 16$  hrs.. Due to symmetry only half of the cross-section was modelled.

Figure 7.7 shows the distribution of the utilization of the splitting tensile strength at  $t = 144$  hrs.. Cracks formed at this time would be through-cracks at the lower part of the wall corresponding to the one observed (cf. Table 6.1). This crack will not close again.

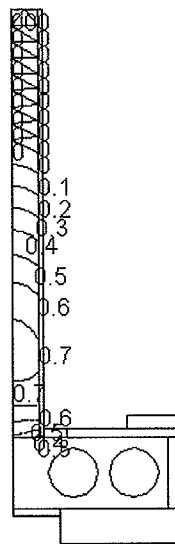


Figure 7.7. Distribution of the ratio between tensile stress and splitting tensile strength at  $t = 144$  hrs.. Due to symmetry only half of the cross-section was modelled. The upper part of the wall is in compression.

The deviation in the curvature at 144 hrs. is due to a too low estimate of the stresses in the wall. If an uniformly distributed tensile stress of the size 0.93 MPa is added to the stresses in the wall, the “missing” curvature can be obtained. Due to the “extra” eigen-



stresses in the wall, the “missing” curvature can be obtained. Due to the “extra” eigenstresses caused by the added “load” the stresses at the critical point will be increased 0.46 MPa. This means the real utilization is approx. 90%.

The “missing” tensile stress in the calculation is probably caused by uncertainties on the material properties and the calculated temperature “load”. If all of the material properties were determined without any uncertainty the size of the “missing” tensile stress corresponds to an “extra” temperature displacement in the cooling phase of 2-3°C. From this point of view the deviation between measured and calculated curvature seems reasonable.

## 8. Conclusion

Based on the test it can be stated that the theoretical assumption of constant curvature is justified when the distance to the end-face exceeds a certain value. In the test this assumption applied at least for the central 3 m of the structure. Therefore it can be concluded that no slip takes place between adjacent structural elements in the intermediate zone of a structure even in the very early age.

The test has shown that the curvature as a function of time can be predicted by use of a non-stationary cross-section calculation. The development of the material properties used are determined as functions of maturity by testing on the actual concrete type (Appendix D).

As the calculation of the curvature is based on a “hardening stress calculation” it can be concluded that the stress development in a typical hardening concrete structure can be predicted.

In the test crack formation was observed at a calculated stress level of approximate 74% of the splitting tensile strength. Due to uncertainties on material properties and calculated temperature “load” the “real” utilization is estimated to 90%.

## 9. Literature

Andersen, M.E. et al.: "HETEK - Control of Early Age Cracking - Phase 8: Modelling of Support Conditions", Danish Road Directorate, Report No. 98, 1997.

DTI Building Technology: "CIMS-2D Ver. 1.1 - User Manual", October 1995.

Pedersen, E.S. et al.: "HETEK - Control of Early Age Cracking in Concrete - Guidelines", Danish Road Directorate, Report No. 120, 1997.

Spange, H. and Pedersen, E.S.: "HETEK - Control of Early Age Cracking in Concrete - Phase 1: Early Age Properties of Selected Concrete", Danish Road Directorate, Report No. 59, 1996.

## **APPENDIX A**

### **Geometry and reinforcement**

## Appendix A Geometry and reinforcement

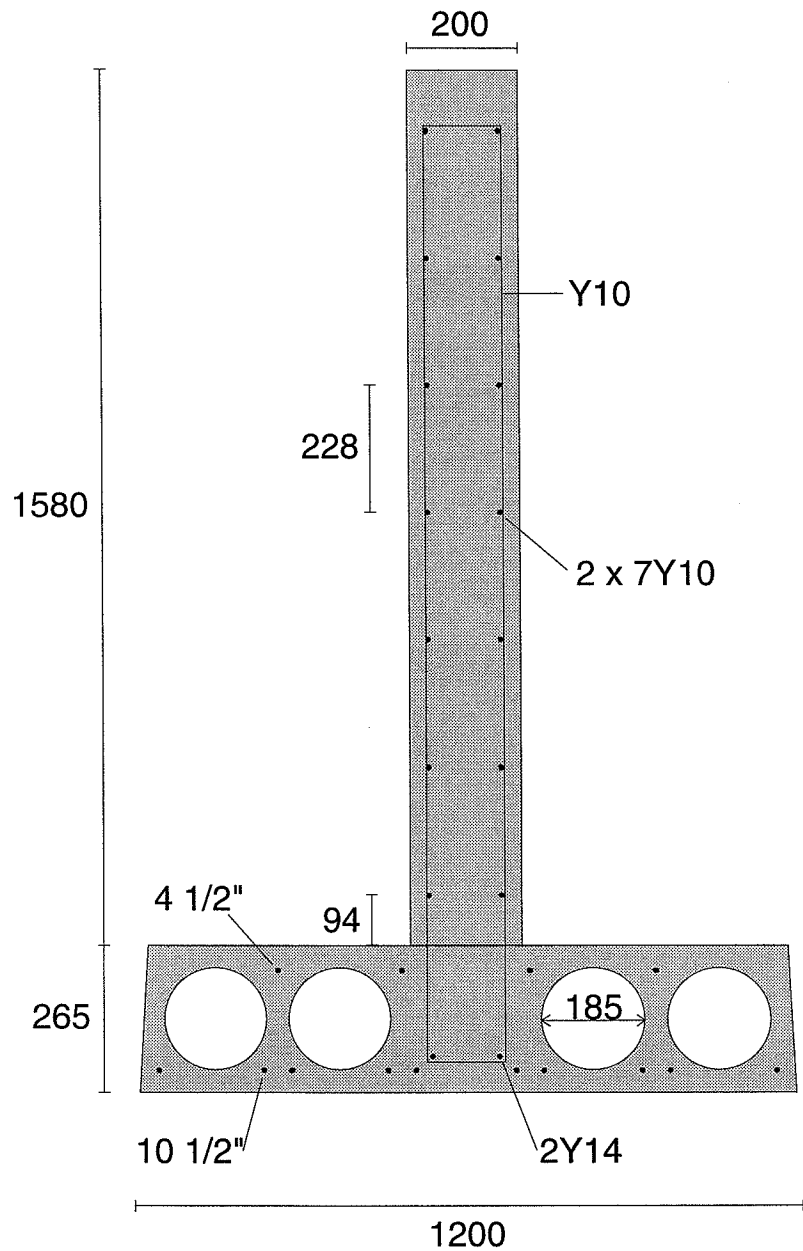


Figure A.1 Cross-section dimensions and reinforcement arrangement. The lines were prestressed with an effective elongation of 6%. The dimensions of the stirrups were 140 x 1695 mm; they were positioned at 200 mm intervals.

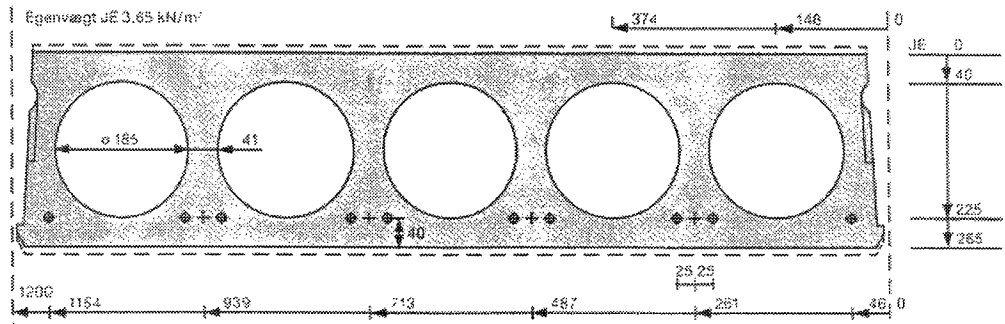


Figure A.2 Geometry of base slab as given in the manufacturer's catalogue. All dimensions in mm. The central core was filled with concrete. The lines at the top of the slab were positioned midway between the cores, 40 mm from the top surface.

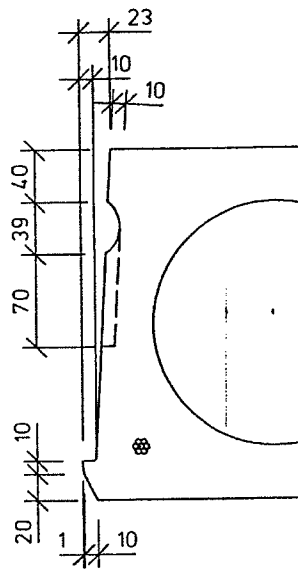


Figure A.: Detail of base slab

## **APPENDIX B**

### **Determining the rigidity of the base slab**

## Appendix B Determining the rigidity of the base

The rigidity determination was carried out 4 days before casting the wall. At that time the base slab was 57 days old.

During the loading test the form was placed on the slab, but not fixed to it. This corresponds to the situation during the hardening test after the wall had set.

The 10 m long slab was simply supported with a span of 8 m and a 1 m cantilever at each end. The slab was supported at one end by two ball-races on each side. The ball-races were placed under the ribs between the hollow cores. At the other end the slab was supported at the centre by a ball-race placed on a roller-bearing.

The deflection figure was measured in relation to a 4.20 m long measuring bridge suspended from the underside of the slab by threaded rods. Measurements were made at 6 points placed at equal distances along the axis as shown in Figure B.1, using electronic movement-transducers. The transducers and their positions are the same as under the hardening test.

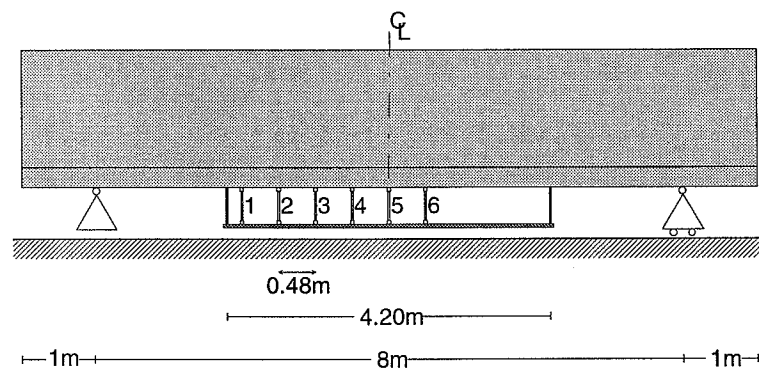


Figure B.1. Sketch of transducer positions. During the test the form was placed on the slab but not fixed to it.

At the central cross-section the structure was subjected to an upward load by means of two interconnected hydraulic jacks placed on each side of the slab. As the jacks were connected, they exert the same force on the slab. The load was measured by an electronic cell placed on one side of the slab (see photo, Figure B.2). The load was applied in 10 steps to a maximum of 19.7 kN.



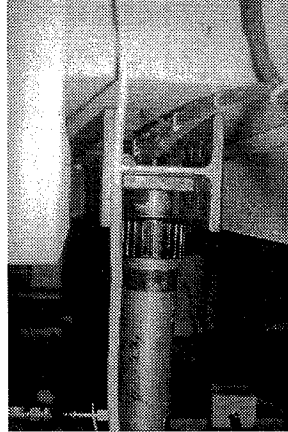


Figure B.2 Photo showing load application

Figure B.3 shows the measured relation between load and deformation for each of the 6 transducers. The deformations are compensated for temperature movements in the transducers as well as in the measuring bridge. The compensation for the temperature movement of the transducers is based on temperature changes measured by means of built-in temperature-sensors. The temperature sensitivity of the transducers varies between  $0.69 \cdot 10^{-5}$  and  $0.75 \cdot 10^{-5}$  m/°C. As the compensation for the temperature movements of the bridge is the same for all six transducers, it has no influence on the shape of the deflection figure and the rigidity determination.

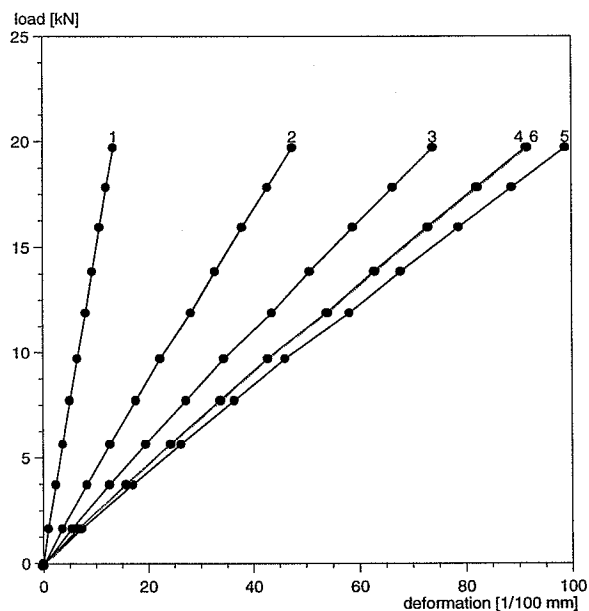


Figure B.3: Relation between measured deformation and applied load for the six transducers. See Figure B.1 for the transducer locations.

The theoretical deflection figure is given by:

$$u(x) = \frac{P \cdot l^3}{16 \cdot E \cdot I} \cdot \left( \frac{x + \frac{1}{2} \cdot l}{l} - \frac{4}{3} \cdot \left( \frac{x + \frac{1}{2} \cdot l}{l} \right)^3 \right) \quad x \leq 0$$

where  $P$  = applied load  
 $l$  = 8 m  
 $I$  =  $1.62 \cdot 10^{-3} \text{ m}^4$   
 $E$  = modulus of elasticity  
 $x$  = distance from the centre

In Figure B.4 the theoretical deflection figure based on  $E = 45000 \text{ MPa}$  is shown together with measured values for selected load steps. The deflections shown are relative to transducer No. 1. It can be seen that there is good agreement between the measured and theoretical deflections.

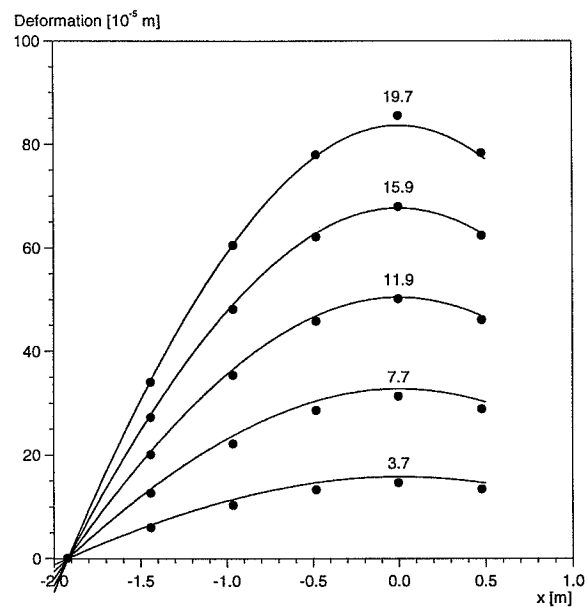


Figure B.4. Measured and theoretical deflections for selected load steps, based on  $E = 45000 \text{ MPa}$ . The deflections are relative to the outermost transducer (No.1).  $x = 0$  corresponds to the central cross-section.

## **APPENDIX C**

### **Measuring the coefficient of thermal expansion**

## **Appendix C            Measuring the coefficient of thermal expansion**

### **C.1 Thermal expansion coefficient of base slab**

The coefficient of thermal expansion was determined on a test specimen cut out of the base slab after the conclusion of the test. The age of the base slab was then 131 days. As the concrete was “old” no shrinkage is assumed to take place during the measuring period of approx. 1 day.

The specimen length is 300 mm and the maximum dimension of the cross-section is less than 150 mm.

The specimen is subjected to a temperature history varying between approx. 14°C and 26°C with a cycle of 12 hrs. The temperature is measured in the center of the specimen. The deformation is measured over a length of 300 mm and compensated for thermal deformations in the measuring equipment. Temperature and deformation are recorded at 5-minute intervals by a datalogger. The measured temperature and the compensated deformation are shown in Figure C.1.

Figure C.2 shows the deformation as function of temperature for the intervals A, B and C marked in Figure C.1. The thermal expansion coefficient is determined by linear regression in these intervals to  $\alpha = 1.01 \cdot 10^{-6} \text{ } ^\circ\text{C}^{-1}$ .

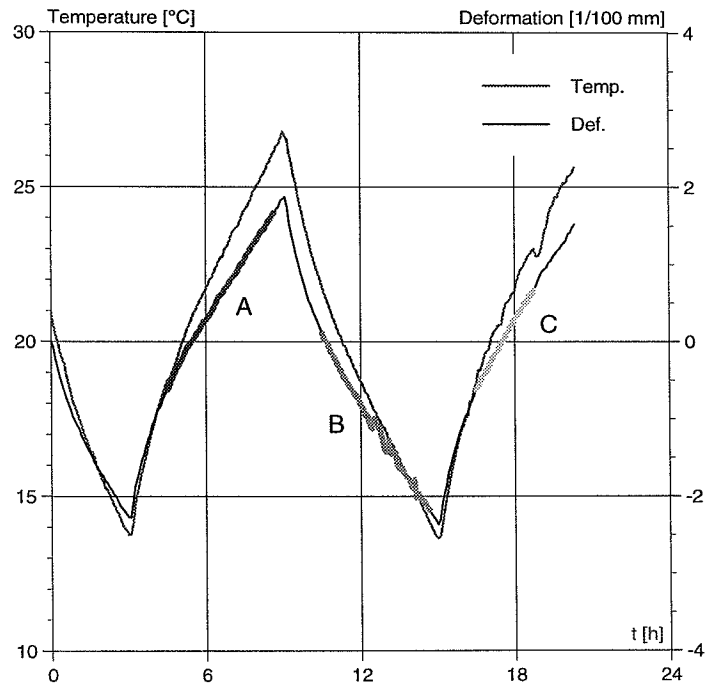


Figure C.1. Base slab. Measured temperature and deformation as function of time. Measuring length = 300 mm.  $t = 0$  at start of measuring.

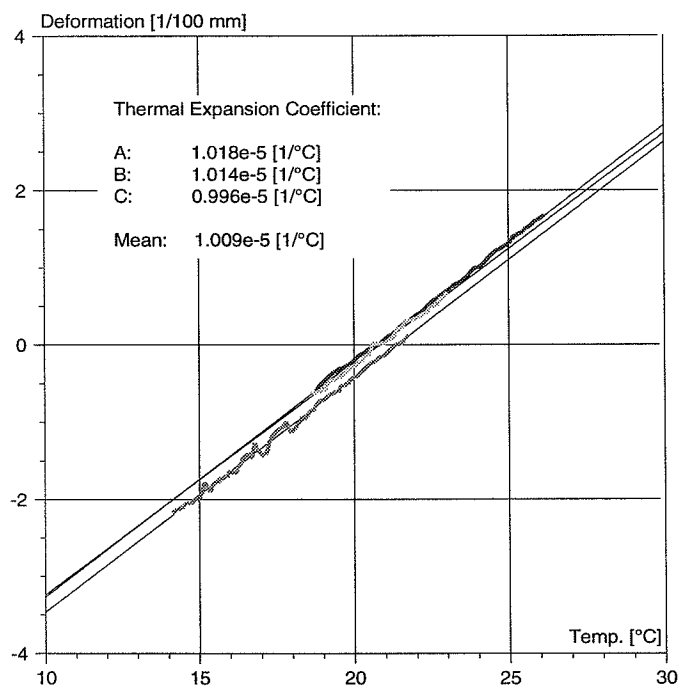


Figure C.2. Base slab. Deformation as function of temperature.

## C.2 Thermal expansion coefficient of wall

The coefficient of thermal expansion as function of maturity was determined on two cylinders D150 x H300 mm casted with the same concrete type as used for the wall (cf. Appendix D). The concrete were supplied by 4K-BETON.

The test specimens were kept sealed during the test.

Specimen No. 1 is subjected to a temperature history varying between approx. 15°C and 26°C with a cycle of 12 hrs.. Specimen No. 2 is kept at a constant temperature of 20°C. The temperatures are measured in the center of the specimens. The deformations are measured over a length of 300 mm and compensated for thermal deformations in the measuring equipment. Temperature and deformation are recorded at 5-minute intervals by a datalogger.

Figure C.3 shows the measured temperatures as function of maturity. Figure C.4 shows the corresponding compensated deformations as function of maturity.

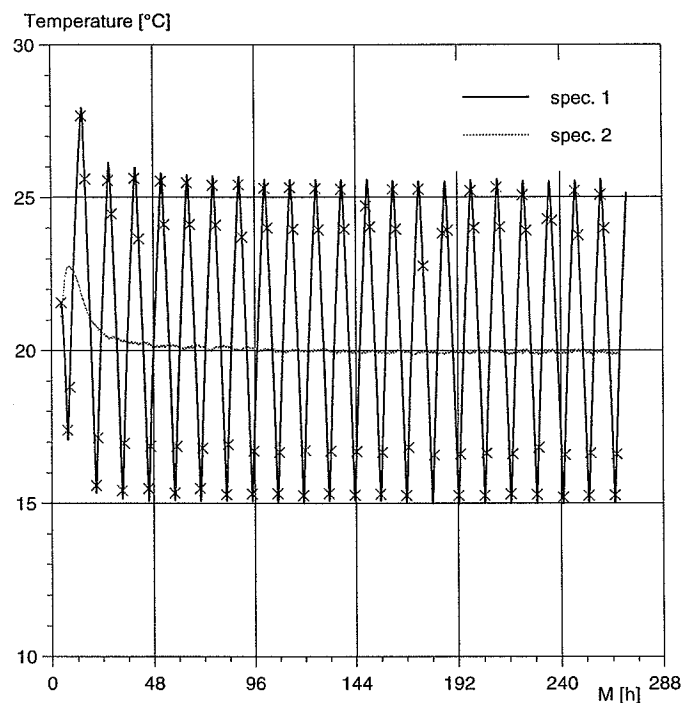


Figure C.3. Wall. Measured temperatures as function of maturity.

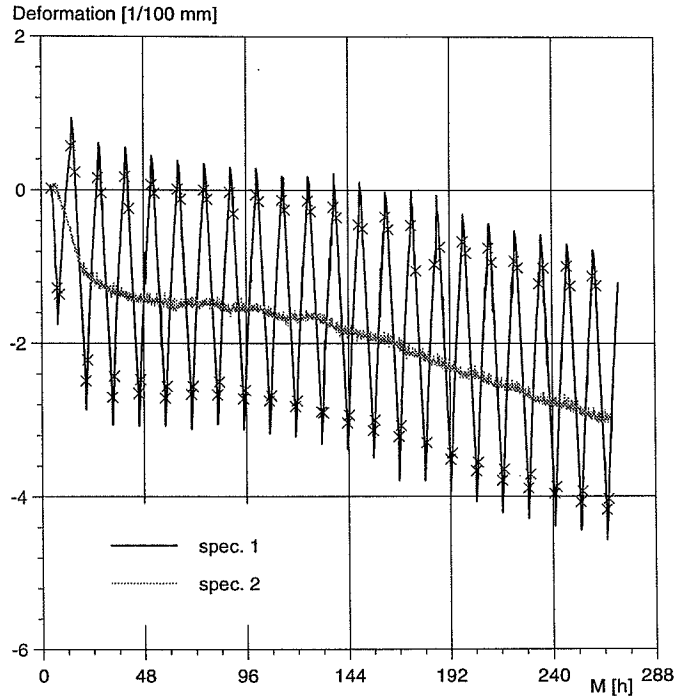


Figure C.4. Wall. Measured deformation compensated for thermal deformation in equipment as function of maturity. Measuring length = 300 mm.

In a given time interval the deformation arises partly from thermal deformation and partly from autogenous shrinkage. The thermal expansion coefficient is assumed to be constant within a given interval of maturity. The autogenous shrinkage is assumed to be described as function of maturity. On the basis of these assumptions the thermal expansion coefficient in a given interval of maturity can be calculated as

$$\alpha = \frac{\Delta\varepsilon_1 - \Delta\varepsilon_2}{\Delta T_1 - \Delta T_2} \quad [^{\circ}\text{C}^{-1}]$$

where

$\Delta\varepsilon_1, \Delta\varepsilon_2$  = change in strain in spec.1 and 2 respectively in the maturity interval considered [m/m]  
 $\Delta T_1, \Delta T_2$  = change in temperature in spec.1 and 2 respectively in the maturity interval considered [ $^{\circ}\text{C}$ ]

The thermal expansion coefficient is determined during heating and cooling in the intervals between the crosses shown in Figure C.3 and C.4. Figure C.5 shows the thermal expansion coefficient as function of maturity.

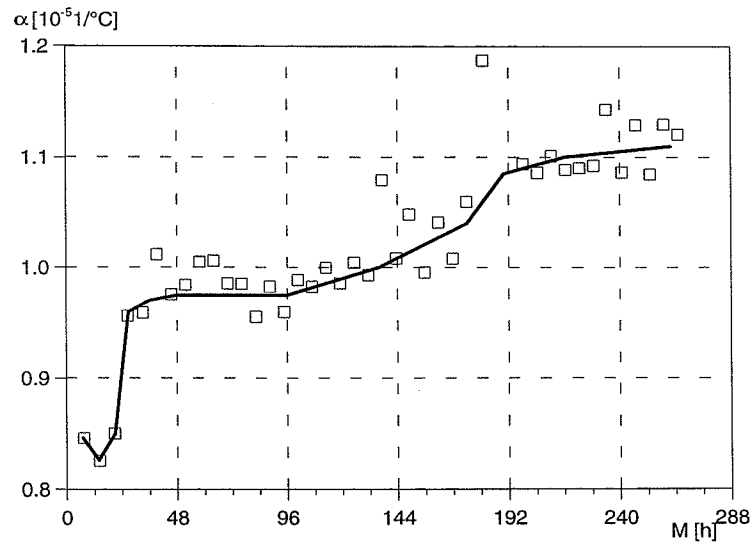


Figure C.5. Thermal expansion coefficient as function of maturity. In the calculation the piecewise linear function given by the line is used.



## **APPENDIX D**

### **Concrete properties**

## Appendix D Concrete properties

The properties of the concrete used for the wall were determined by previous performed testing as described in [Spange and Pedersen, 1996]. The heat development, however, was determined on the actual concrete batch used in the test. The thermal expansion coefficient was determined by subsequent testing.

### D.1 Mix design

Mix design	Type/origin/class	kg/m <sup>3</sup>	
Cement	Low-alkali Sulfatresistant CEM I 42,5(HS/EA/≤2)	285	1)
Flyash	Danaske	60	1)
Silica fume	Elkem	12	2)
Water	Water	127	3)
Fine aggregate	RN, Avedøre sand 0/4, SA	758	4)
Coarse aggregate	Rønne granite 8/16, A	535	4)
	Rønne granite 16/25, A	565	4)
Air entrainment	Conplast 316 AEA	0,357	5)
Plasticiser	Conplast 212	1,428	6)
Superplasticiser	Peramin F	2,856	7)

Tabel D.1. Mix design

- 1) Dry
- 2) Silica fume, slurry. The quantity corresponds to dry silica fume. The amount of water is included in the 127 kg/m<sup>3</sup> of water.
- 3) Added water + free water content of aggregates + water content of silica fume, slurry. The quantity of water does not include the water content of plasticizer and air entrainment.
- 4) Water-saturated surface - dry.
- 5) The quantity includes water content (95 % of the stated value).
- 6) The quantity includes water content (64 % of the stated value).
- 7) The quantity includes water content (66 % of the stated value).

### D.2 Properties of fresh concrete

Temperature, slump, air content and density were measured just after arrival at DTI approx. 0.8 hrs. after mixing.

Temperature	=	19.5 °C
Slump	=	115 mm
Air content	=	5.4 %
Density	=	2388 kg/m <sup>3</sup>

### D.3 Thermal properties

The thermal conductivity is assumed to be  $8 \text{ kJ/m/h/}^\circ\text{C}$  independent of maturity.

The specific heat is assumed to be  $1 \text{ kJ/kg/}^\circ\text{C}$  independent of maturity. The density used in temperature calculation is  $2328 \text{ kg/m}^3$  corresponding to the density measured in the previous performed testing.

The heat development as function of maturity is determined by testing on the actual concrete batch. The result is shown in Figure D.1. In the calculation the measured heat development is used and not the curve determined by regression.

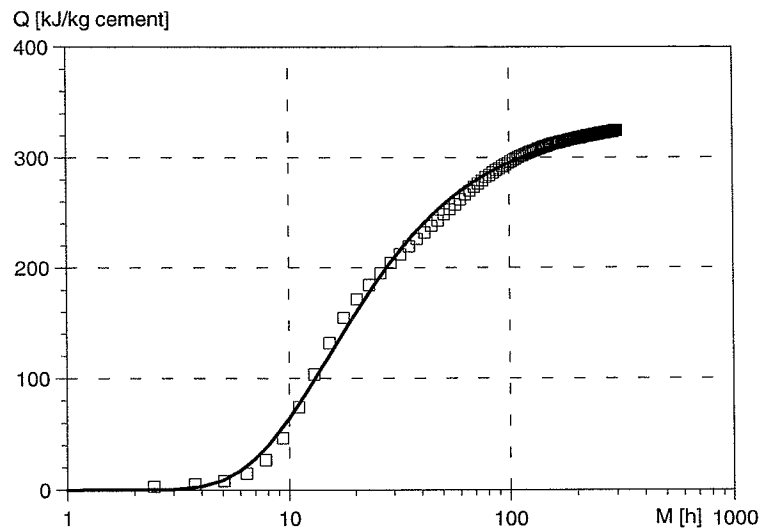


Figure D.1. Heat development per kg cement determined on the actual concrete batch. Cement content =  $287.6 \text{ kg/m}^3$ . The parameters determined by regression are:  $Q_\infty = 332 \text{ kJ/kg cement}$ ,  $\tau_e = 14.43 \text{ h}$ ,  $\alpha = 1.15$ . In the calculation the measured curve is used and not the regression.

#### D.4 Mechanical properties

The thermal expansion coefficient as a function of maturity was determined by subsequent testing as described in Appendix C. The thermal expansion coefficient used in the calculation is shown in Figure D.2.

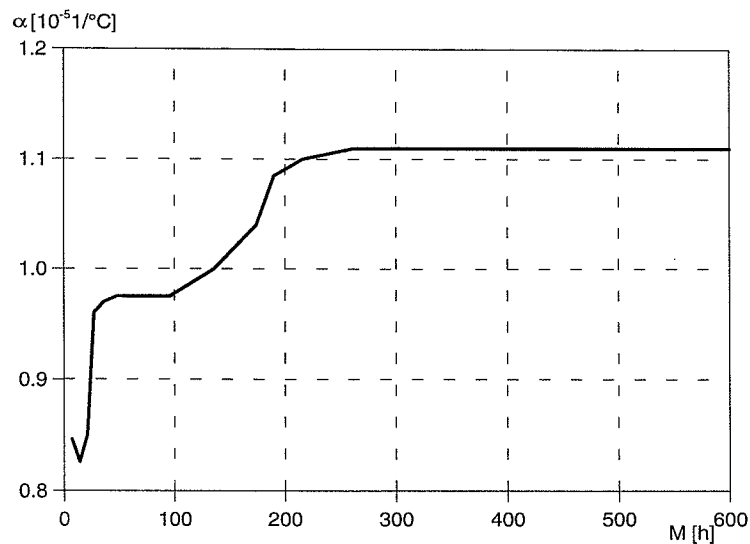


Figure D.2. Thermal expansion coefficient used in calculation (cf. Appendix C).

The modulus of elasticity as a function of maturity was determined by previous performed testing as

$$E(M) = 34327 \cdot \exp\left(-\left(\frac{12.89}{M}\right)^{1.5}\right)$$

The creep properties as function of maturity are determined by previous performed testing. The creep model used can be described as a serial connection between a dashpot and a parallel connection of a dashpot and a spring. In this model the external dashpot represents the irreversible part of the creep while the parallel connection represents the reversible part. The model corresponds to the model described in [Pedersen, 1997]. The parameters used in the calculation are shown in Table D.2.

Property	Function	a	b	c	d
$\eta_1$ [MPa hours]	$a+b \cdot \exp\left[-\left(\frac{c}{M}\right)^d\right]$	$0.177 \cdot 10^7$	$0.1975 \cdot 10^9$	1438	0.562
$\eta_2$ [MPa hours]	$a \cdot \exp(b \cdot M)$	$0.2382 \cdot 10^6$	$0.4163 \cdot 10^{-2}$	-	-
$E_2$ [MPa]	$a \cdot \exp(b \cdot M)$	$0.1302 \cdot 10^6$	$0.1222 \cdot 10^{-2}$	-	-

Table D.2. Parameters of creep model described in [Pedersen, 1997].

$\eta_1$  is the viscosity of the external dashpot

$\eta_2$  is the viscosity of the dashpot in the parallel connection

$E_2$  is the spring constant

The autogenous shrinkage as a function of maturity was determined by previous performed testing. In the calculation the autogenous shrinkage shown in Figure D.3 is used.

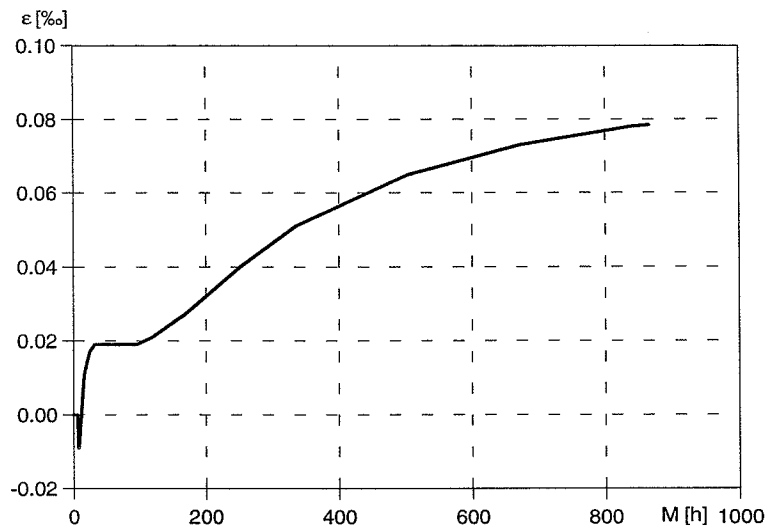


Figure D.3. Autogenous shrinkage as function of maturity.

The splitting tensile strength as a function of maturity was determined by previous performed testing. The calculated stresses are compared with the splitting tensile strength given by

$$\sigma_{sp}(M) = 3.7 \cdot \exp\left(-\left(\frac{29.22}{M}\right)^{0.77}\right)$$

## **APPENDIX E**

### **Placing of thermo-sensors**

## Appendix E Placing of thermosensors

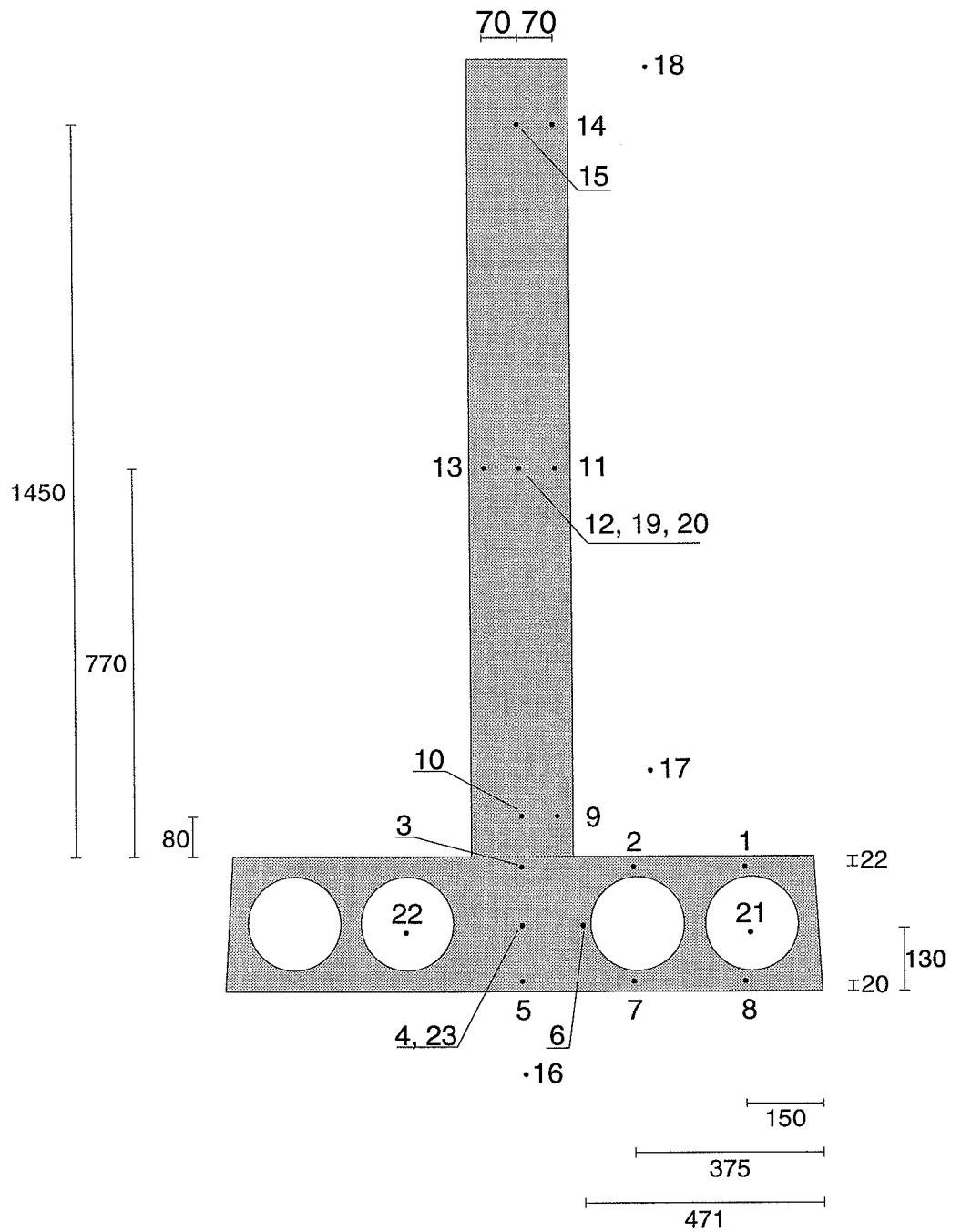


Figure E.1: Placing of thermo-sensors. Sensors 1 - 18 are placed at the central section. Sensor 19 is placed 1 m from the centre. Sensor 20 is placed 2 m from one end. Sensor 23 is placed 2.4 m from the centre.

## **APPENDIX F**

### **Measured and calculated concrete temperatures**



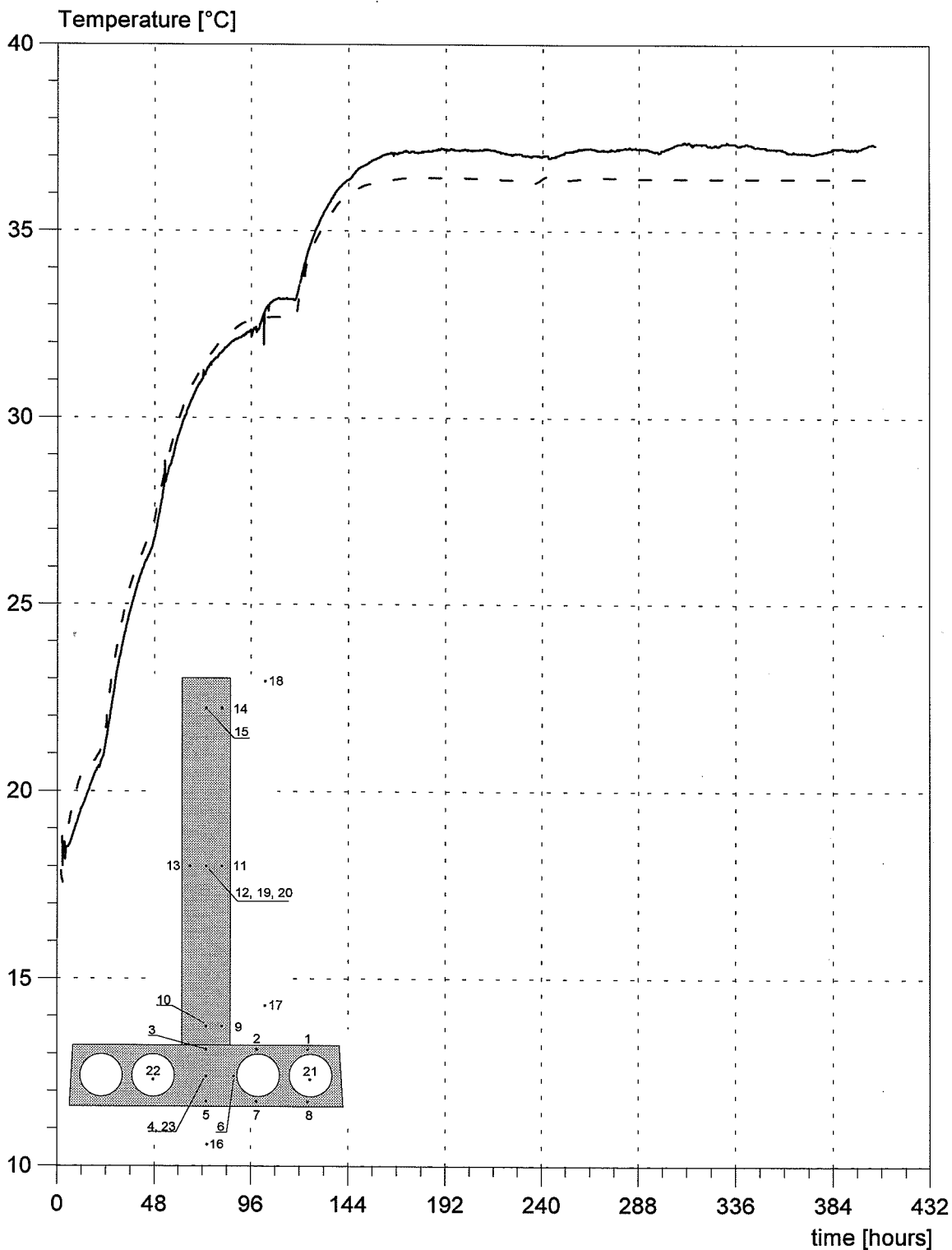
DTI Building Technology  
 Gregersensvej, 2630 Taastrup

Concrete Temperature  
 thermocouple no. 1

Client: HETEK 3 + 4  
 Name: Stage 7

Ref.: 53459  
 Date: 02/28/97

Init.: HSP/ESP



t = 0 at time of mixing  
 Start of measurings at end of casting

— measured - no. 1  
 - - - calculated - no. 1

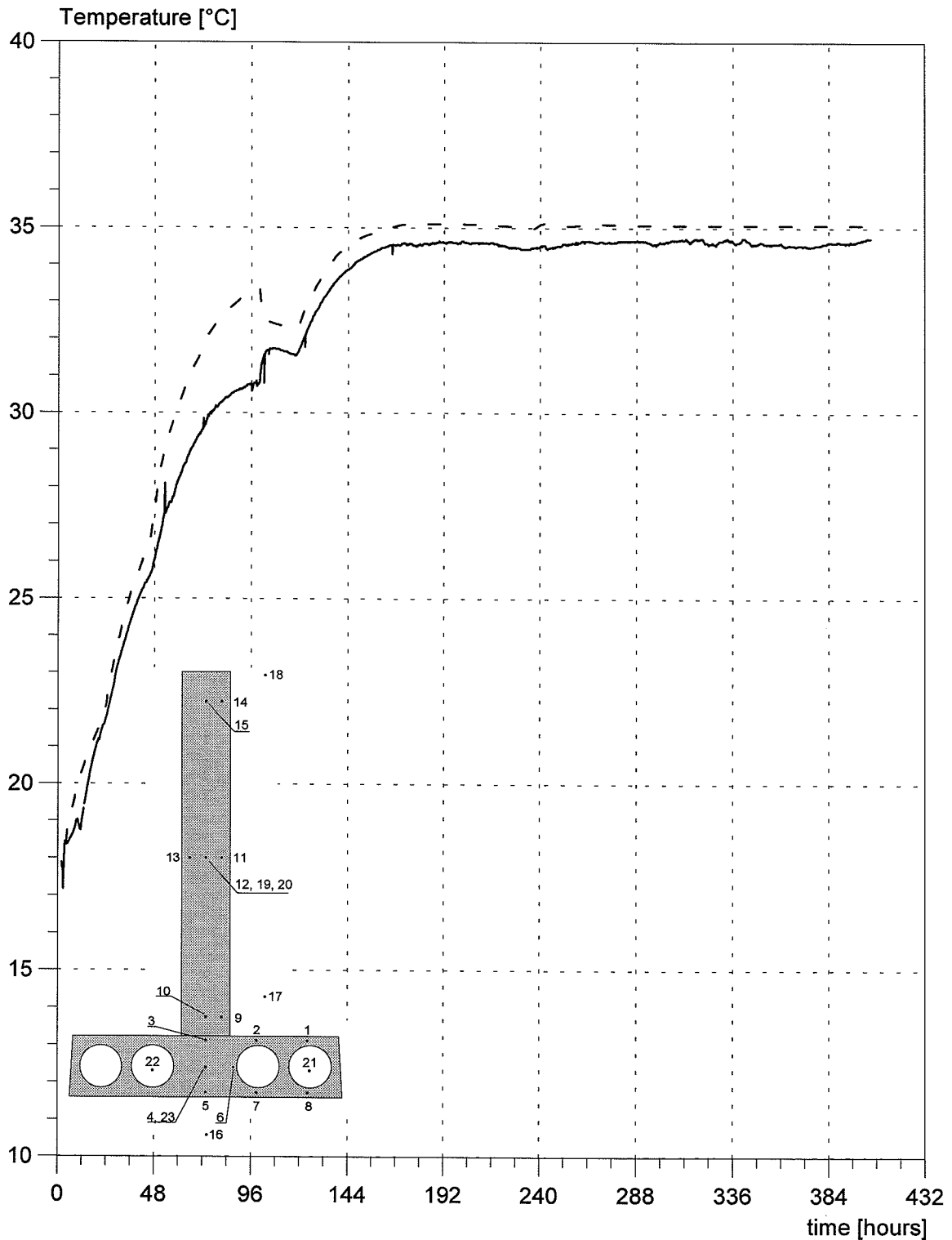
DTI Building Technology  
 Gregersensvej, 2630 Taastrup

Concrete Temperature  
 thermocouple no. 2

Client: HETEK 3 + 4  
 Name: Stage 7

Ref.: 53459  
 Date: 02/28/97

Init.: HSP/ESP



t = 0 at time of mixing  
 Start of measurings at end of casting

— measured - no. 2  
 - - - calculated - no. 2

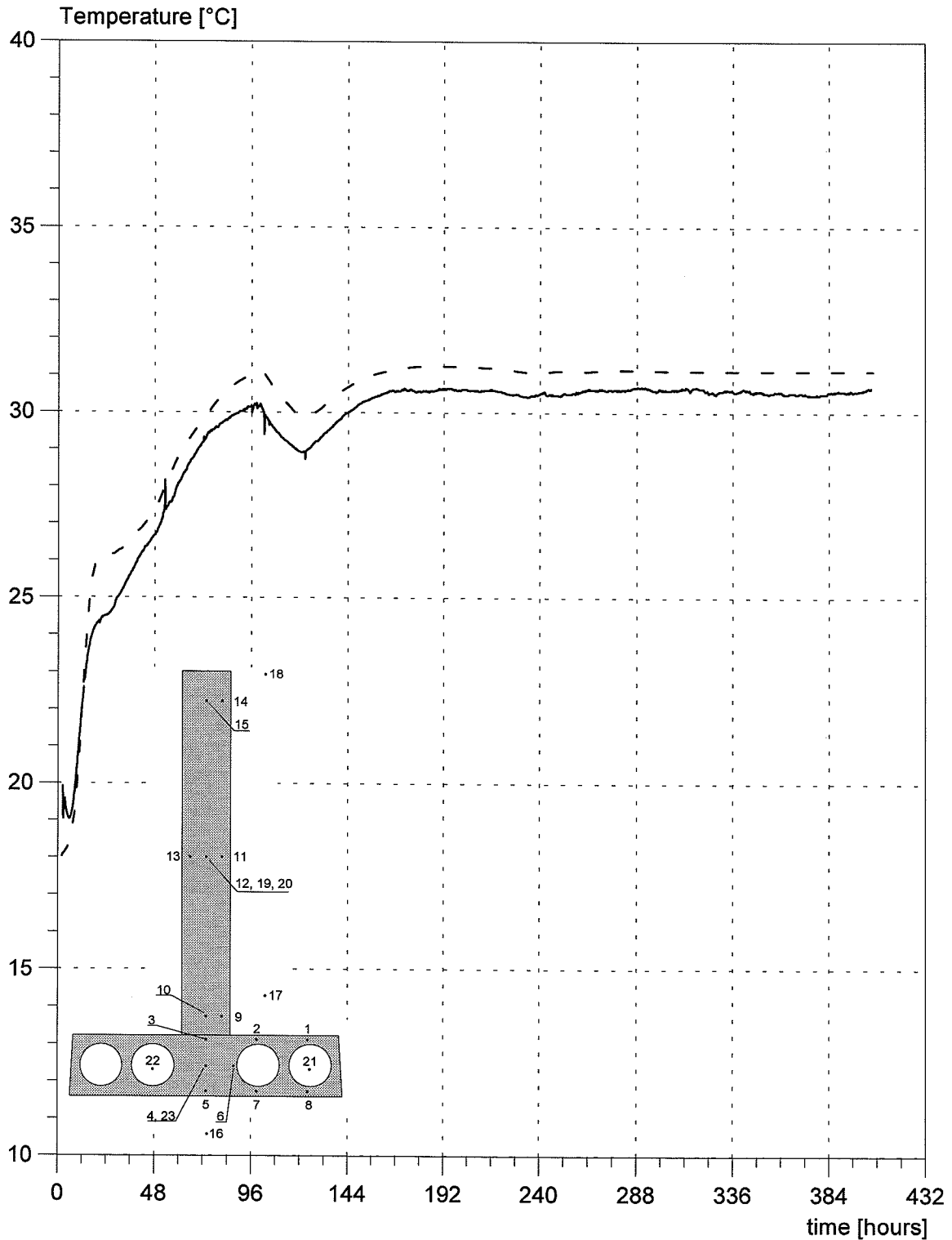
DTI Building Technology  
 Gregersensvej, 2630 Taastrup

Concrete Temperature  
 thermocouple no. 3

Client: HETEK 3 + 4  
 Name: Stage 7

Ref.: 53459  
 Date: 02/28/97

Init.: HSP/ESP



t = 0 at time of mixing  
 Start of measurings at end of casting

— measured - no. 3  
 - - - calculated - no. 3

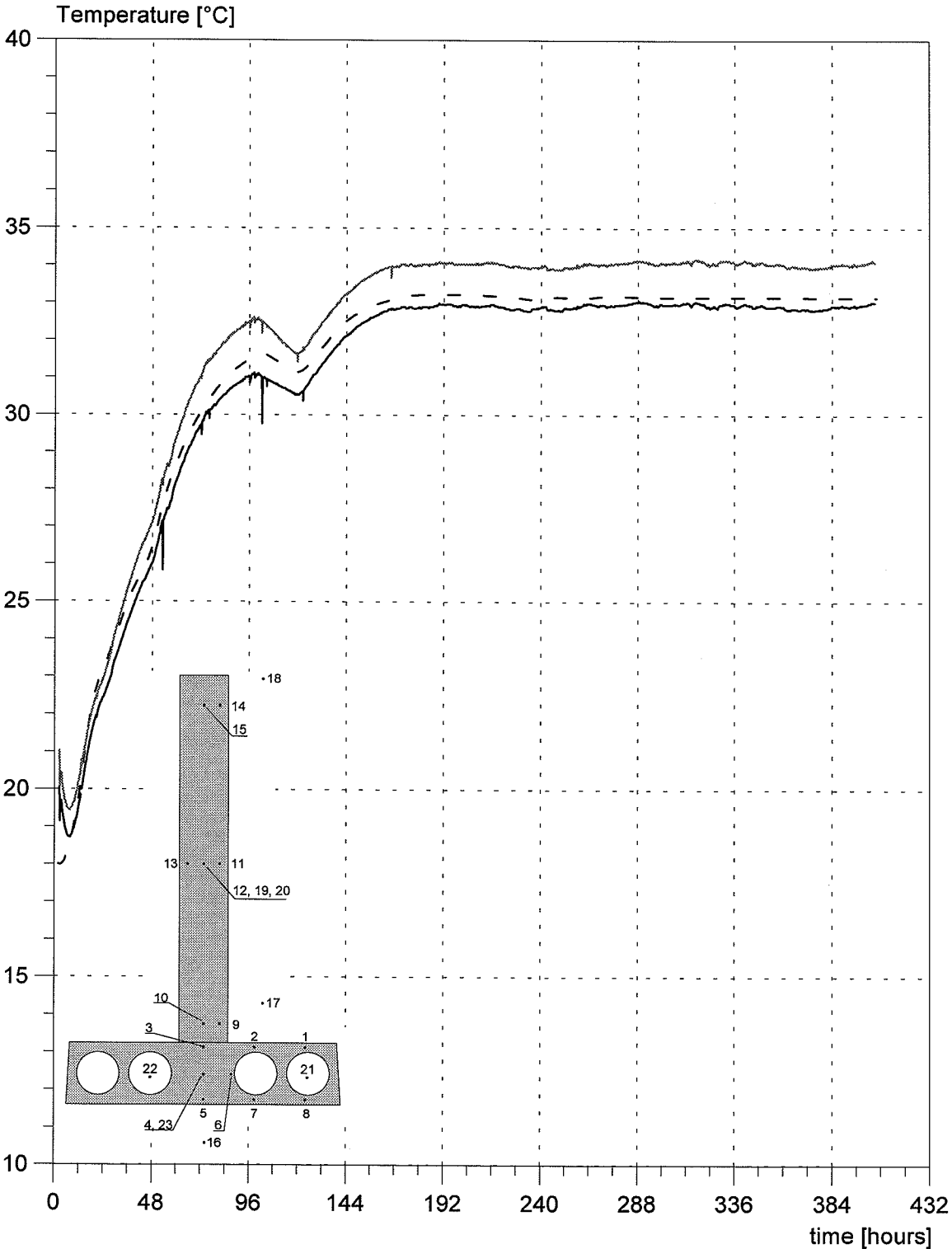
DTI Building Technology  
Gregersensvej, 2630 Taastrup

Concrete Temperature  
thermocouple no. 4 & 23

Client: HETEK 3 + 4  
Name: Stage 7

Ref.: 53459  
Date: 02/28/97

Init.: HSP/ESP



t = 0 at time of mixing  
Start of measurings at end of casting

- measured - no. 4
- measured - no. 23
- - - calculated

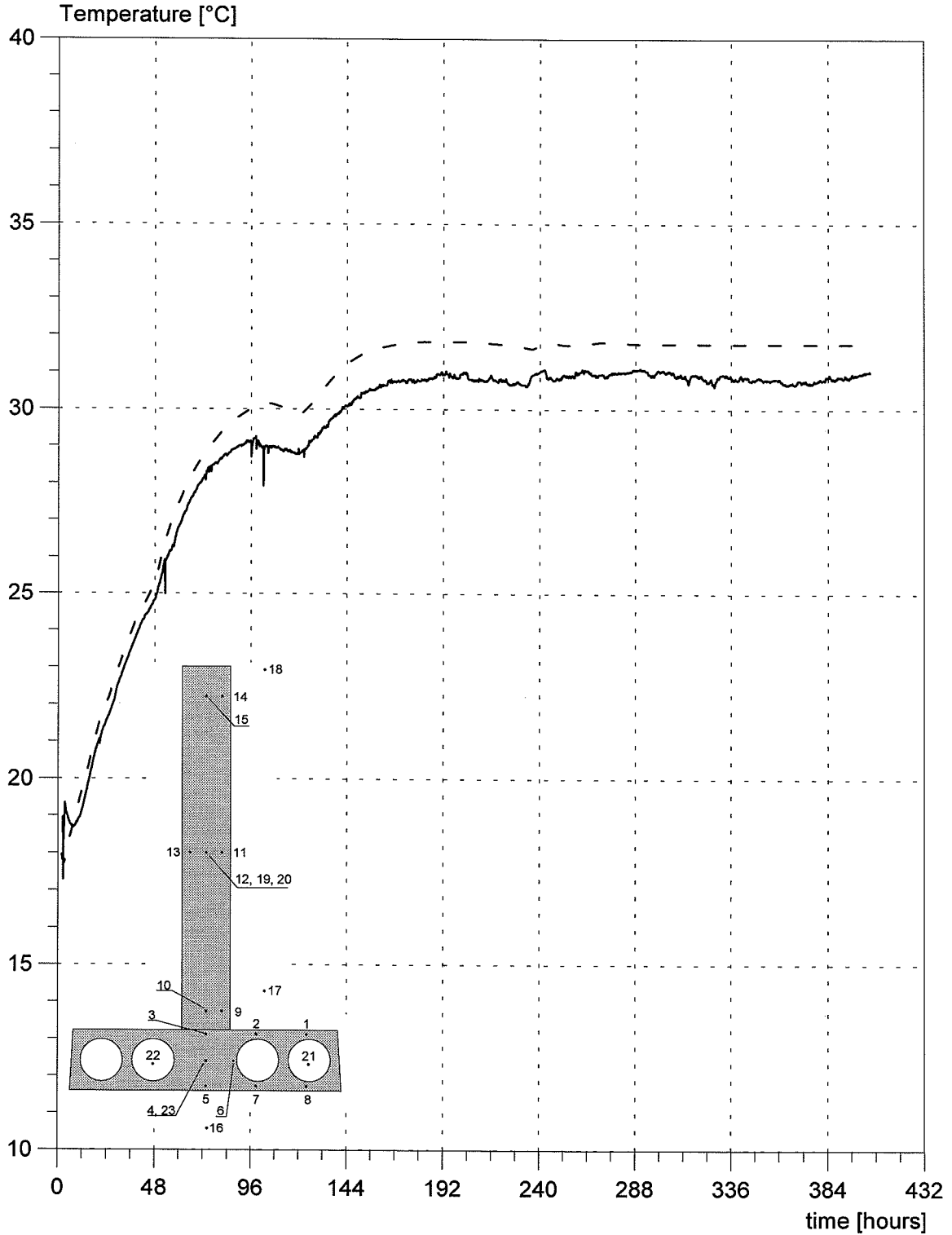
DTI Building Technology  
 Gregersensvej, 2630 Taastrup

Concrete Temperature  
 thermocouple no. 5

Client: HETEK 3 + 4  
 Name: Stage 7

Ref.: 53459  
 Date: 02/28/97

Init.: HSP/ESP



t = 0 at time of mixing  
 Start of measurings at end of casting

— measured - no. 5  
 - - - calculated - no. 5

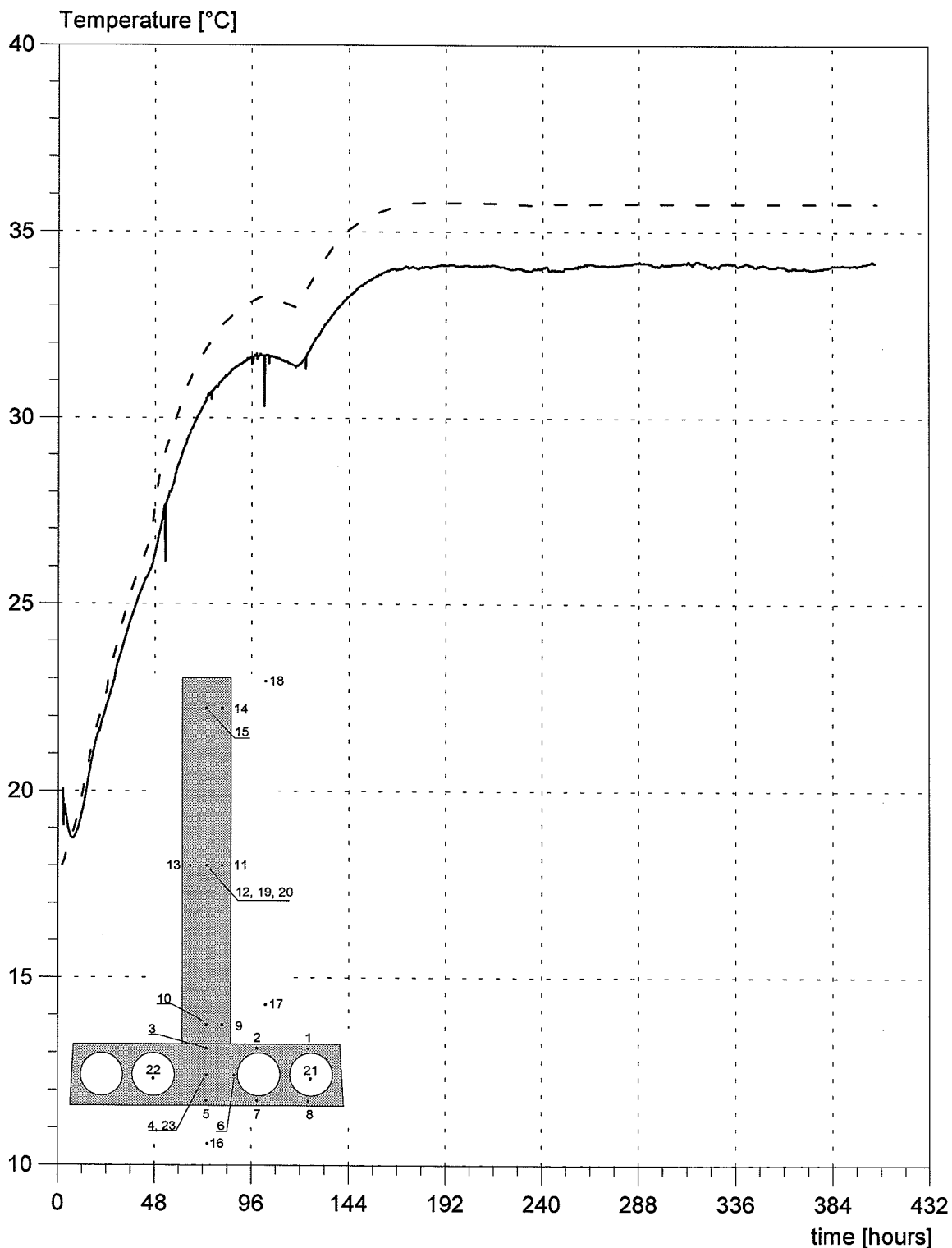
DTI Building Technology  
 Gregersensvej, 2630 Taastrup

Concrete Temperature  
 thermocouple no. 6

Client: HETEK 3 + 4  
 Name: Stage 7

Ref.: 53459  
 Date: 02/28/97

Init.: HSP/ESP



t = 0 at time of mixing  
 Start of measurings at end of casting

— measured - no. 6  
 - - - calculated - no. 6

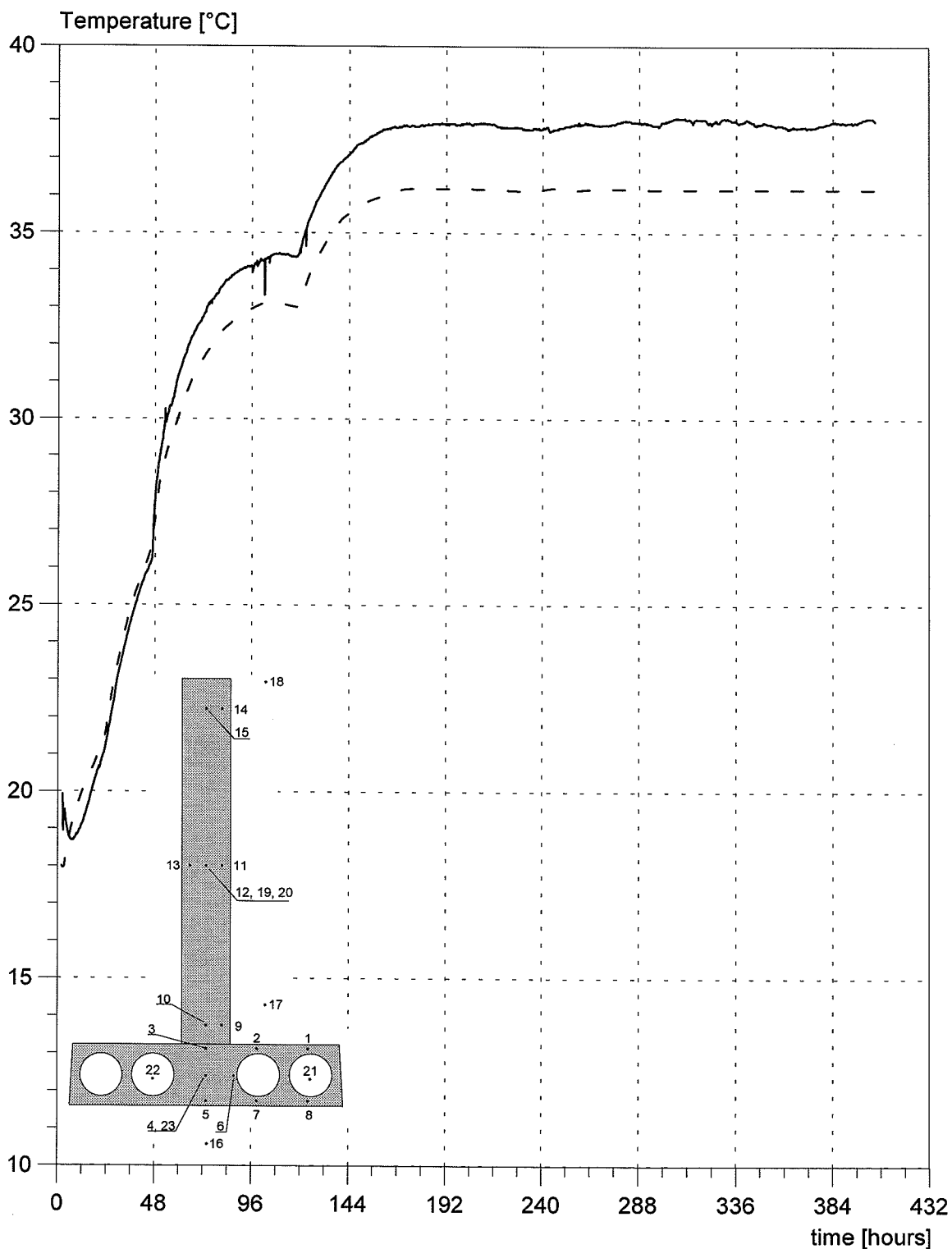
DTI Building Technology  
 Gregersensvej, 2630 Taastrup

Concrete Temperature  
 thermocouple no. 7

Client: HETEK 3 + 4  
 Name: Stage 7

Ref.: 53459  
 Date: 02/28/97

Init.: HSP/ESP



t = 0 at time of mixing  
 Start of measurings at end of casting

— measured - no. 7  
 - - - calculated - no. 7

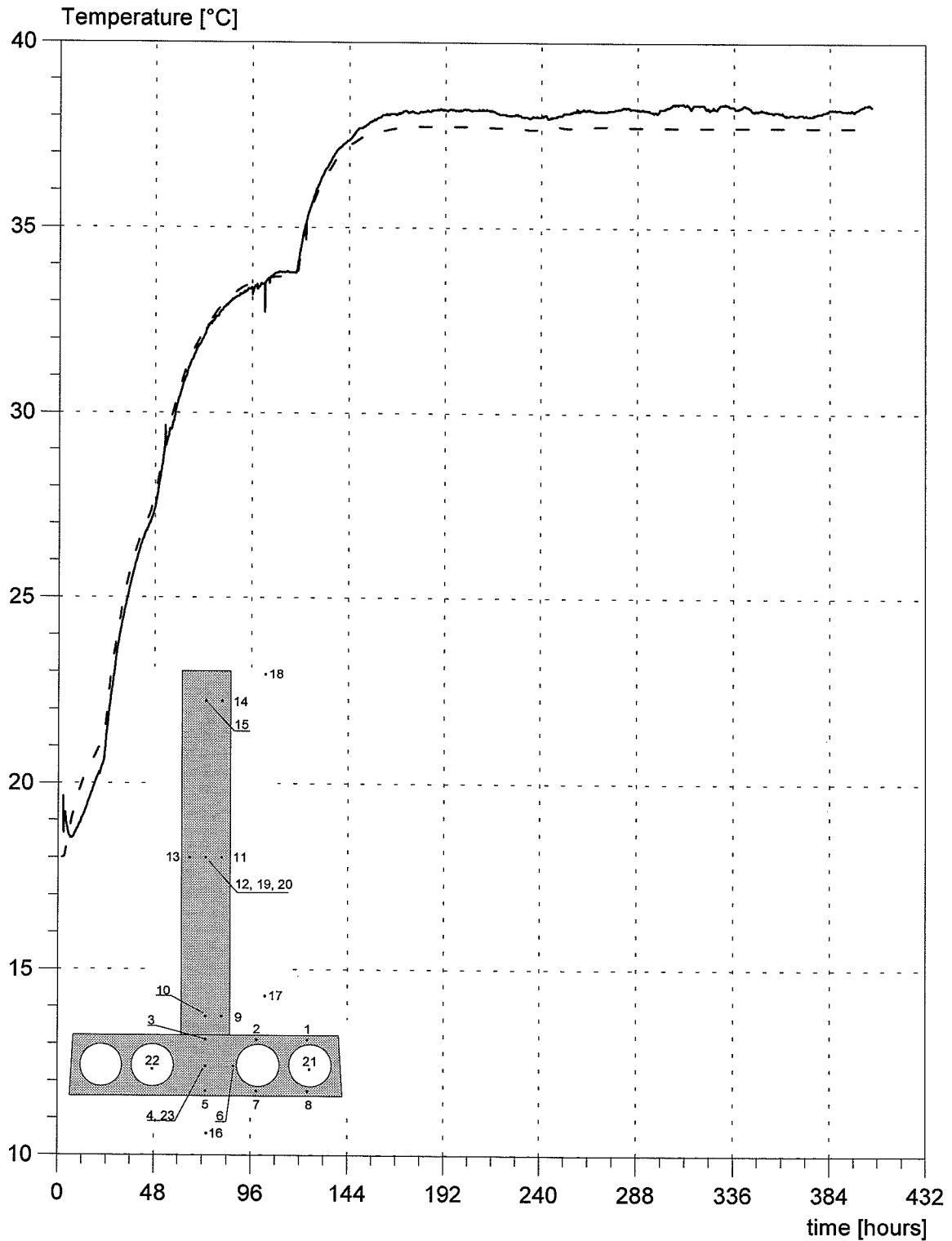
DTI Building Technology  
 Gregersensvej, 2630 Taastrup

Concrete Temperature  
 thermocouple no. 8

Client: HETEK 3 + 4  
 Name: Stage 7

Ref.: 53459  
 Date: 02/28/97

Init.: HSP/ESP



t = 0 at time of mixing  
 Start of measurings at end of casting

— measured - no. 8  
 - - - calculated - no. 8



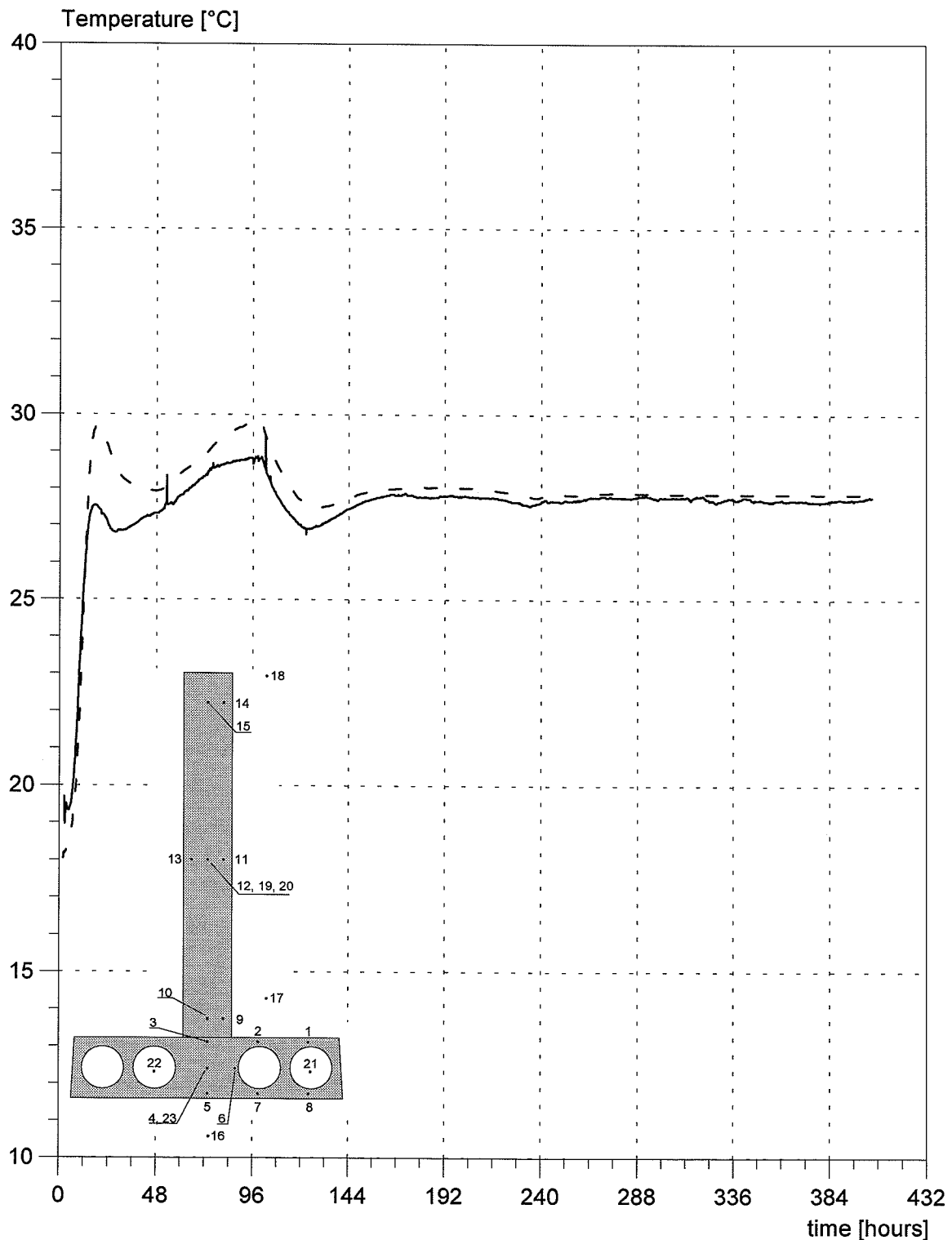
DTI Building Technology  
Gregersensvej, 2630 Taastrup

Concrete Temperature  
thermocouple no. 9

Client: HETEK 3 + 4  
Name: Stage 7

Ref.: 53459  
Date: 02/28/97

Init.: HSP/ESP



t = 0 at time of mixing  
Start of measurings at end of casting

— measured - no. 9  
- - - calculated - no. 9

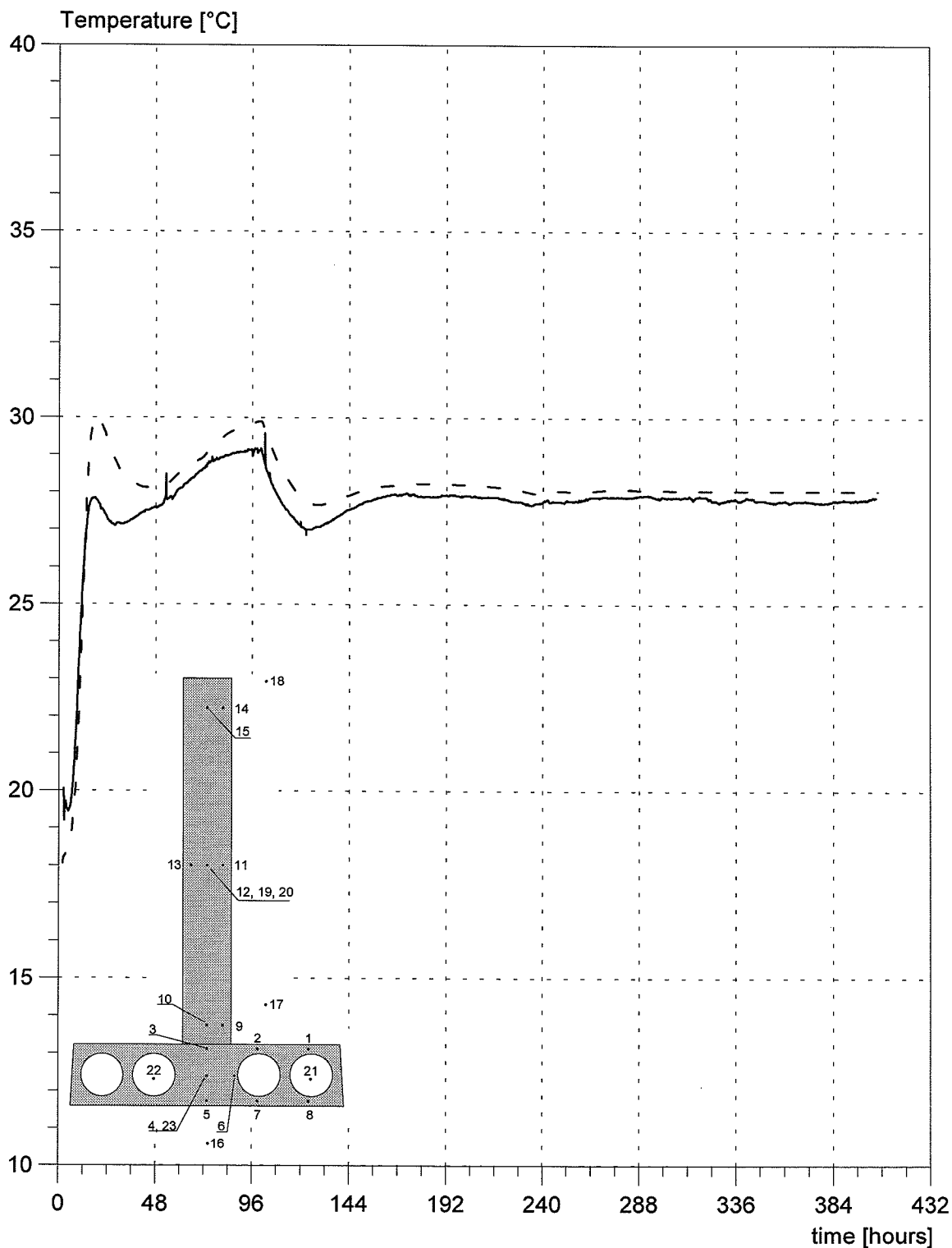
DTI Building Technology  
 Gregersensvej, 2630 Taastrup

Concrete Temperature  
 thermocouple no. 10

Client: HETEK 3 + 4  
 Name: Stage 7

Ref.: 53459  
 Date: 02/28/97

Init.: HSP/ESP



t = 0 at time of mixing  
 Start of measurings at end of casting

— measured - no. 10  
 - - - calculated - no. 10

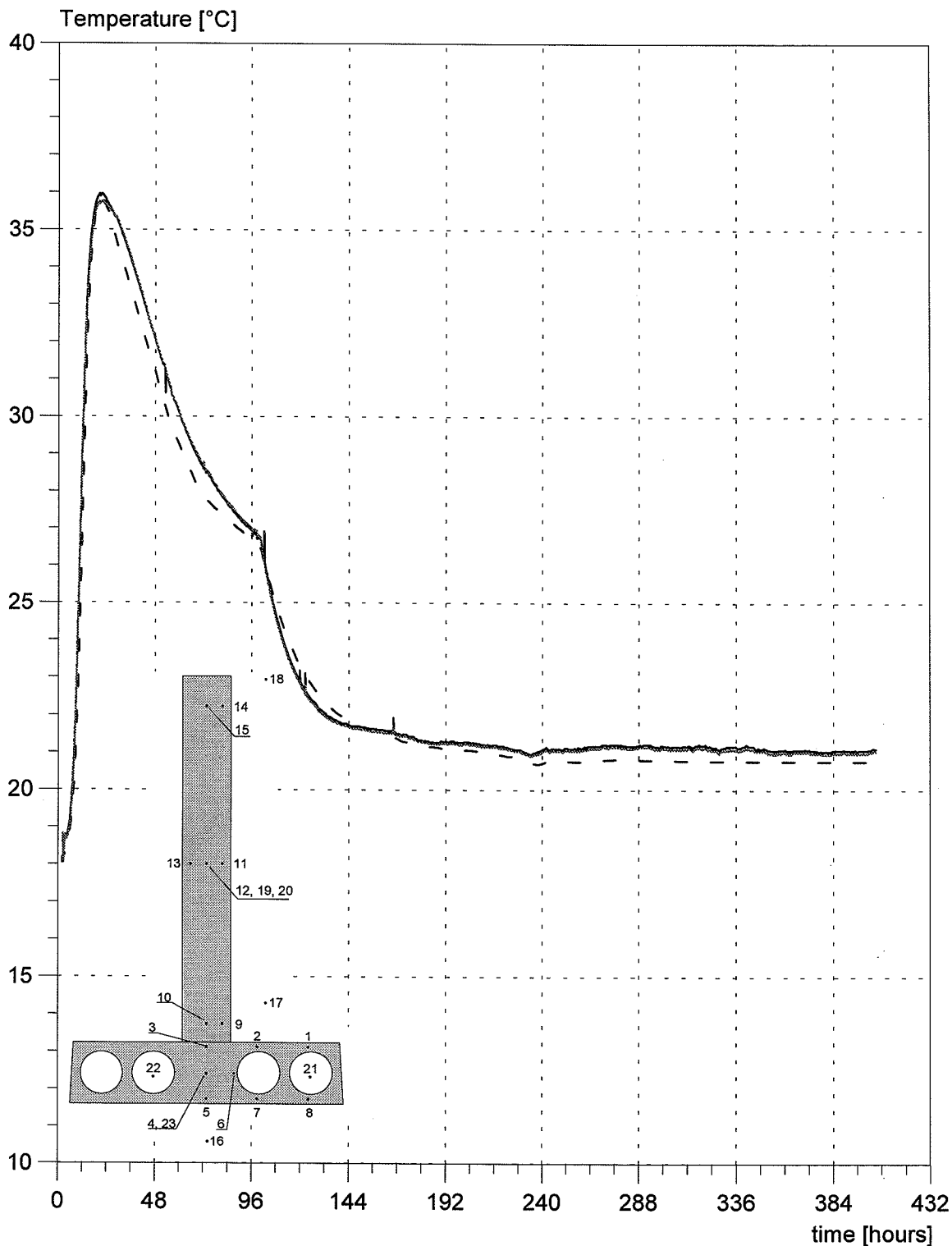
DTI Building Technology  
 Gregersensvej, 2630 Taastrup

Concrete Temperature  
 thermocouple no. 11, 13

Client: HETEK 3 + 4  
 Name: Stage 7

Ref.: 53459  
 Date: 02/28/97

Init.: HSP/ESP



t = 0 at time of mixing  
 Start of measurings at end of casting

- measured - no. 11
- measured - no. 13
- - - calculated - no. 11, 13

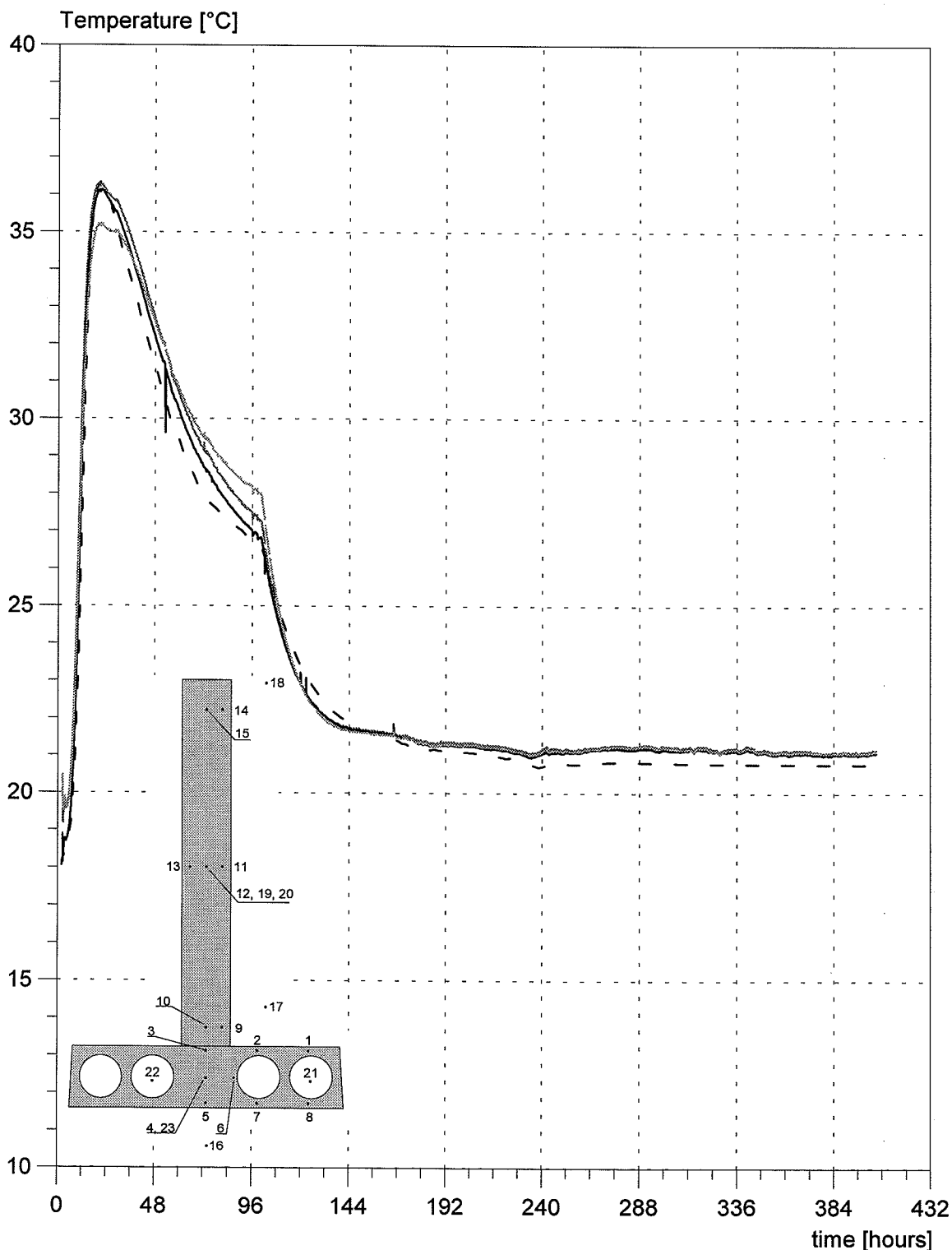
DTI Building Technology  
 Gregersensvej, 2630 Taastrup

Concrete Temperature  
 thermocouple no. 12, 19 & 20

Client: HETEK 3 + 4  
 Name: Stage 7

Ref.: 53459  
 Date: 02/28/97

Init.: HSP/ESP



t = 0 at time of mixing  
 Start of measurings at end of casting

- measured - no. 12
- measured - no. 19
- measured - no. 20
- - calculated - no. 12

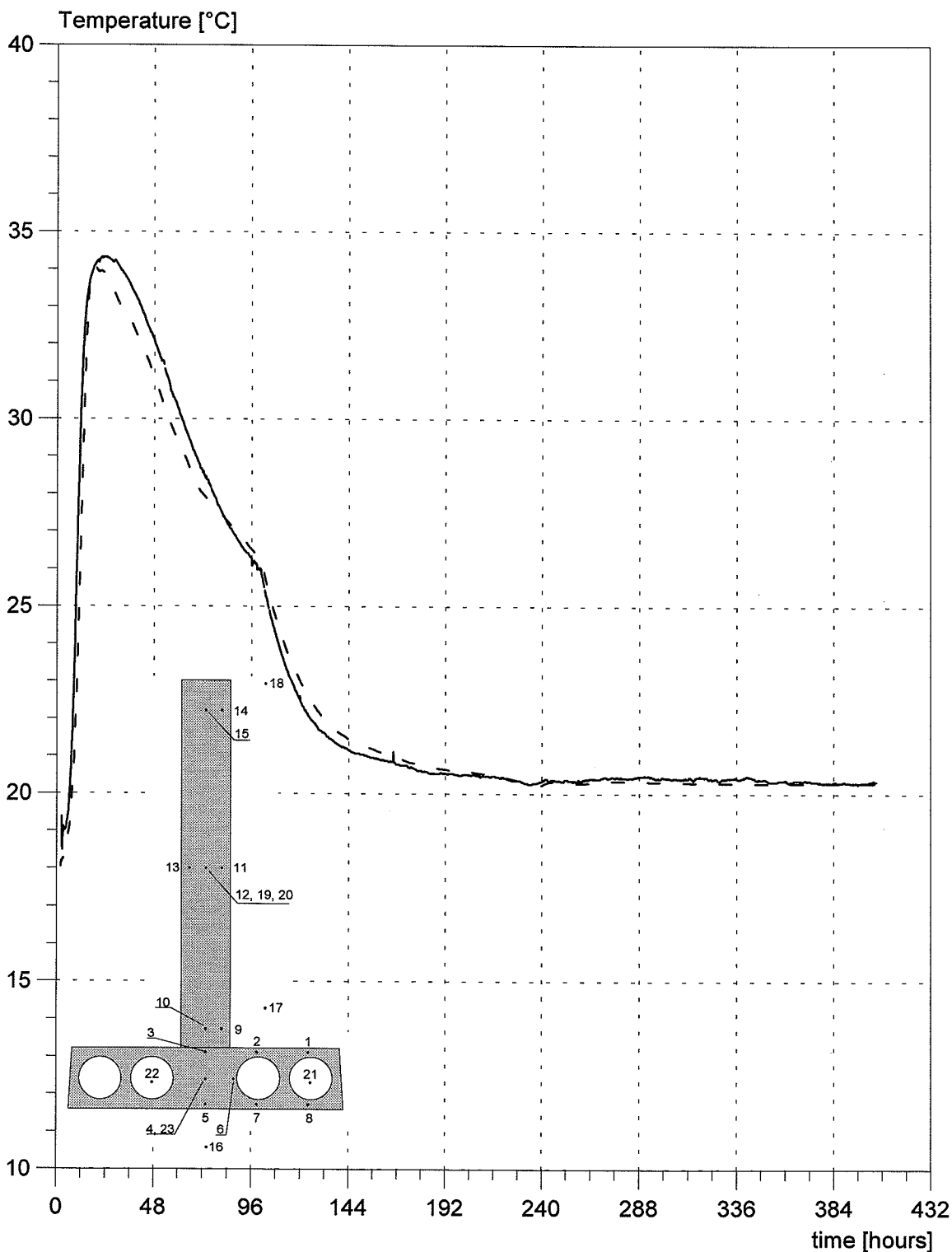
DTI Building Technology  
 Gregersensvej, 2630 Taastrup

Concrete Temperature  
 thermocouple no. 14

Client: HETEK 3 + 4  
 Name: Stage 7

Ref.: 53459  
 Date: 02/28/97

Init.: HSP/ESP



t = 0 at time of mixing  
 Start of measurings at end of casting

— measured - no. 14  
 - - - calculated - no. 14

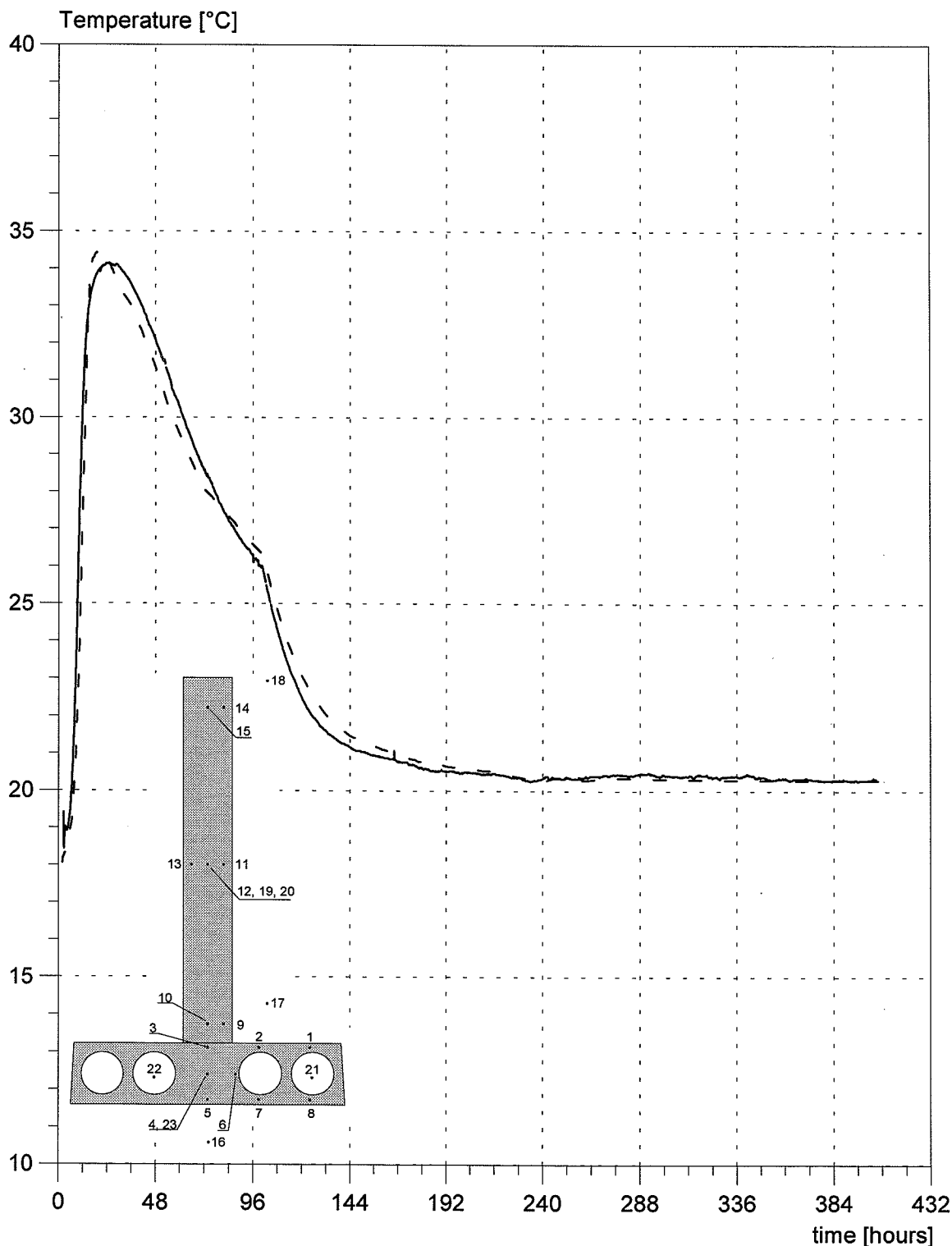
DTI Building Technology  
 Gregersensvej, 2630 Taastrup

Concrete Temperature  
 thermocouple no. 15

Client: HETEK 3 + 4  
 Name: Stage 7

Ref.: 53459  
 Date: 02/28/97

Init.: HSP/ESP



t = 0 at time of mixing  
 Start of measurings at end of casting

— measured - no. 15  
 - - - calculated - no. 15

## **APPENDIX G**

### **Measured Air Temperatures**

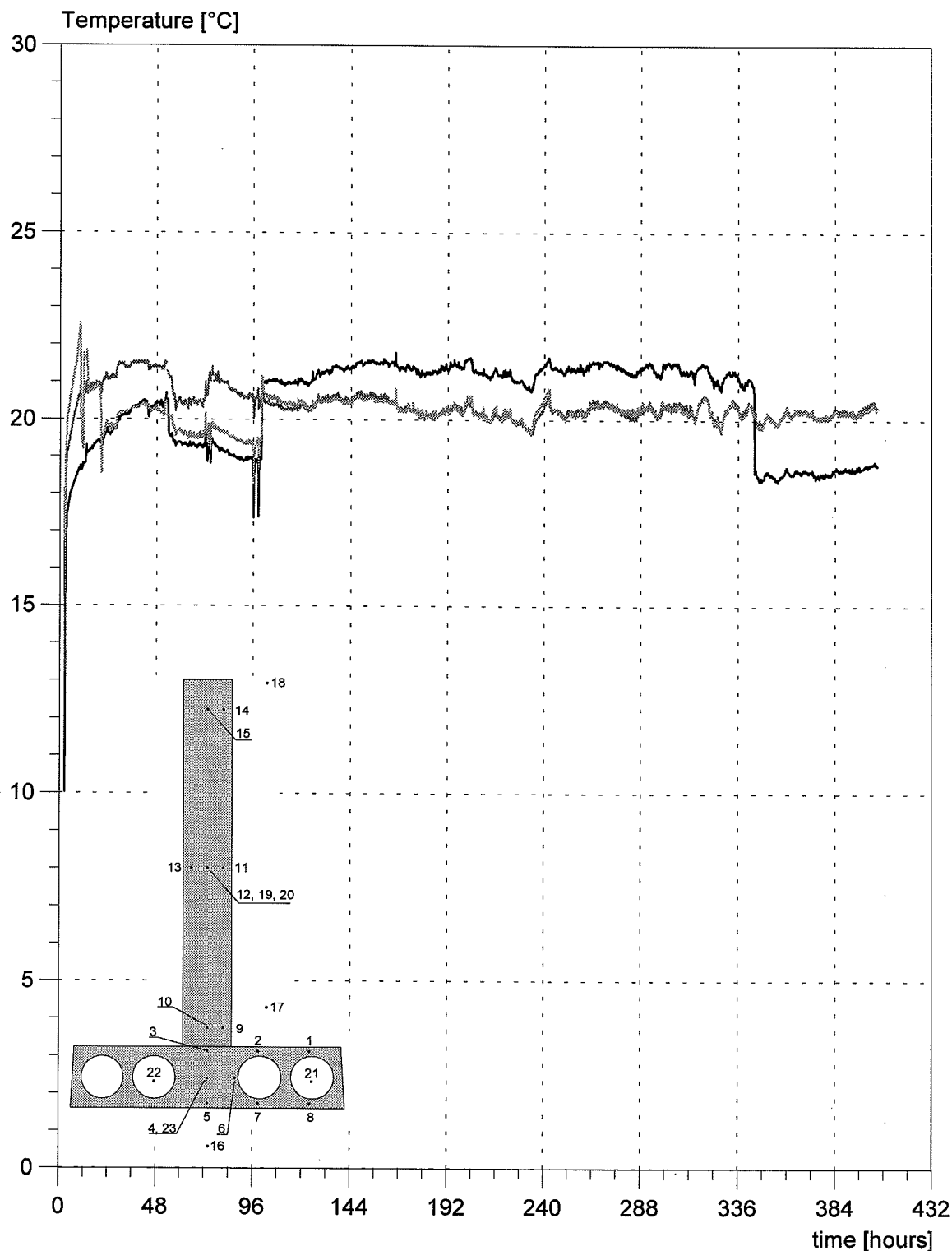
DTI Building Technology  
Gregersensvej, 2630 Taastrup

Air Temperature  
thermocouple no. 16, 17 & 18

Client: HETEK 3 + 4  
Name: Stage 7

Ref.: 53459  
Date: 02/25/97

Init.: HSP/ESP



$t = 0$  at time of mixing  
Start of measurements at end of casting

Thermocouple no. 16 was fallen down in the periods 54-100 h  
and 345 h to end of test.

Thermocouple no. 17 was fallen down in the period 25-100 h

Thermocouple no. 18 was fallen down in the period 54-100 h

— measured - no. 16  
- - - measured - no. 17  
... measured - no. 18



## **APPENDIX H**

### **Measured temperatures in the hollow cores of the base slab**

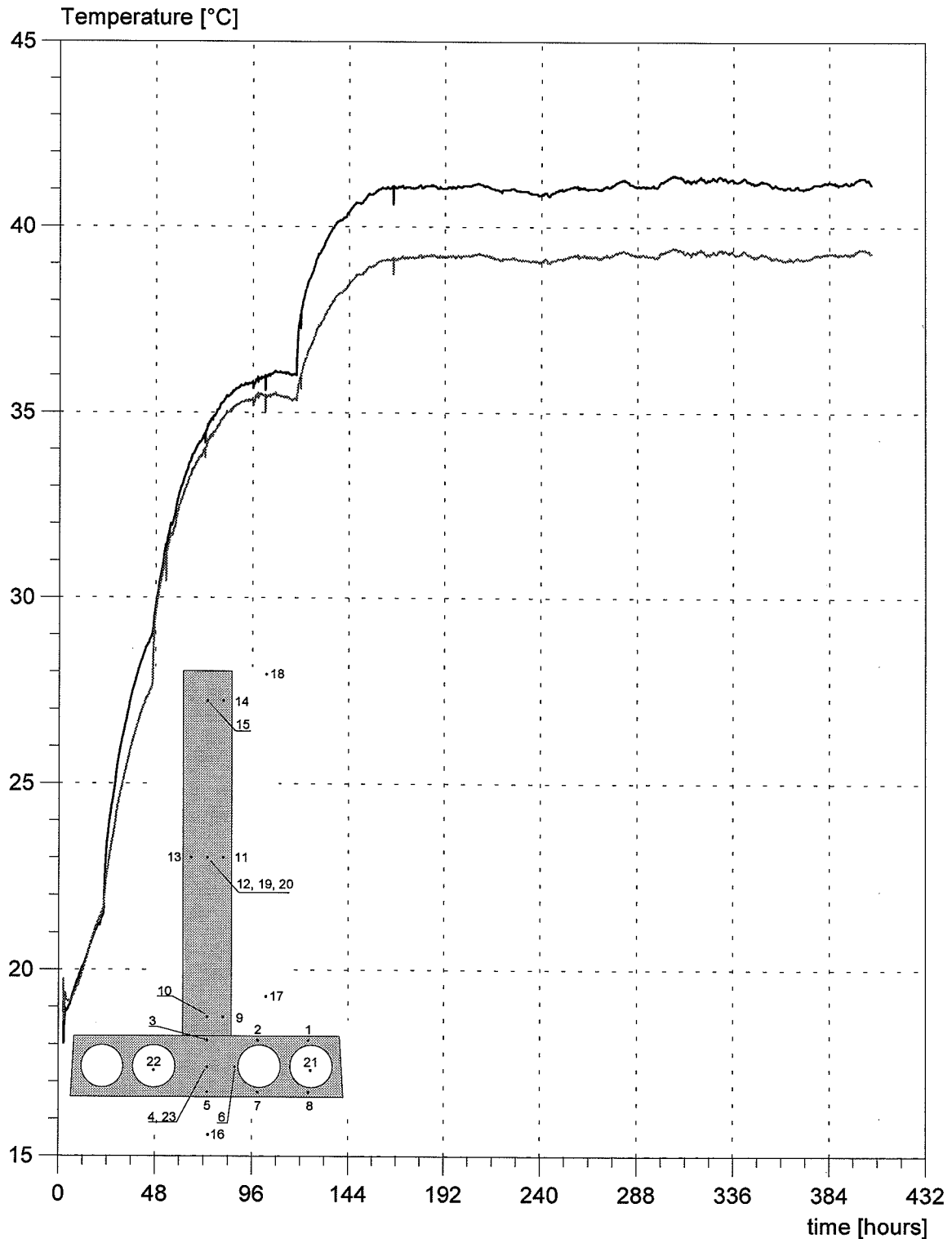
DTI Building Technology  
 Gregersensvej, 2630 Taastrup

Air Temperature  
 thermocouple no. 21 & 22

Client: HETEK 3 + 4  
 Name: Stage 7

Ref.: 53459  
 Date: 02/25/97

Init.: HSP/ESP



t = 0 at time of mixing  
 Start of measurings at end of casting

— measured - no. 21  
 - - - measured - no. 22

## **APPENDIX I**

### **Measured deformations relative to the measuring bridge**

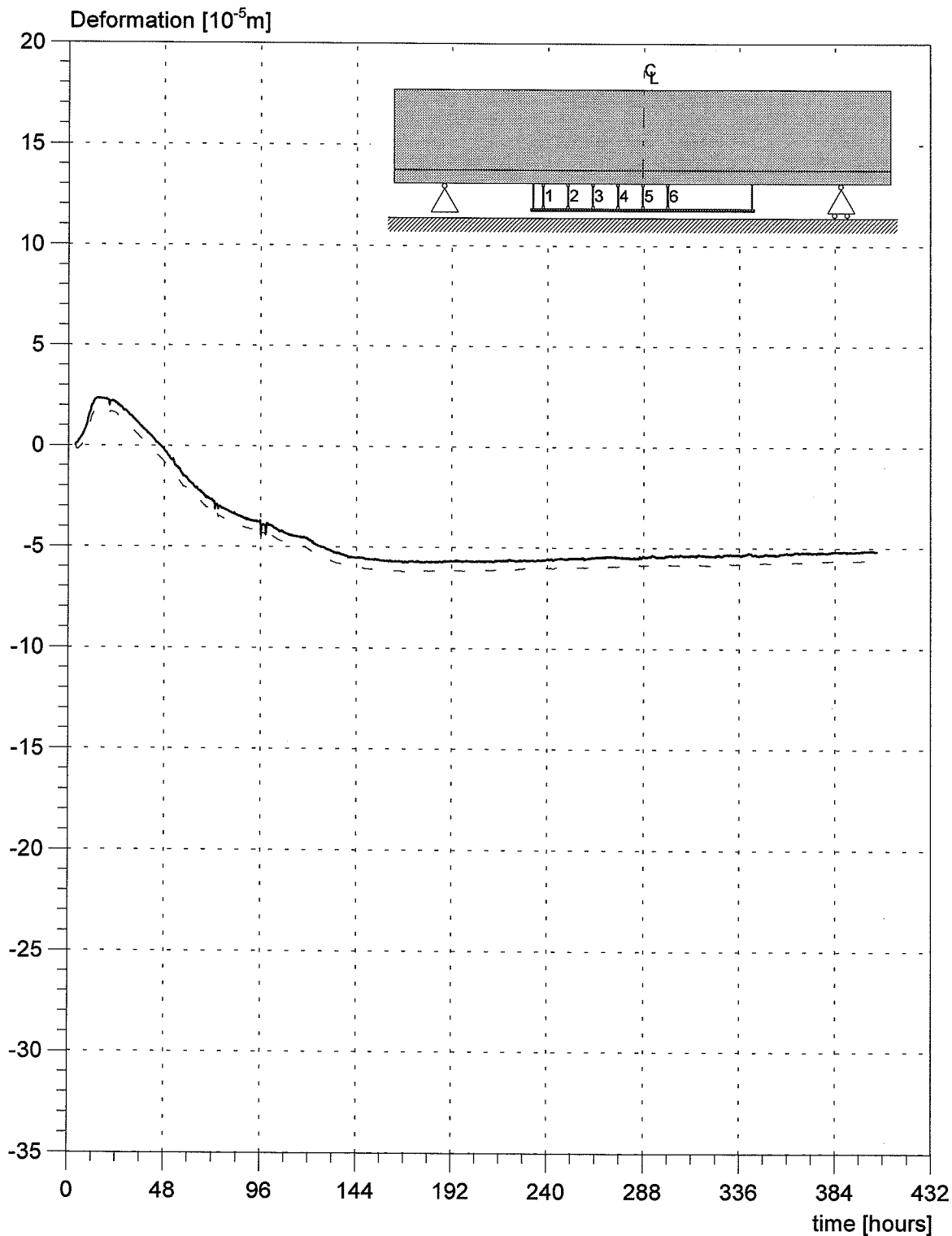
DTI Building Technology  
 Gregersensvej, 2630 Taastrup

Vertical deformation  
 transducer no. 1

Client: HETEK 3 + 4  
 Name: Stage 7

Ref.: 53459  
 Date: 02/25/97

Init.: HSP/ESP



t = 0 at time of mixing  
 Start of measurings at t=3.499 h

— temp. compensated  
 - - measured

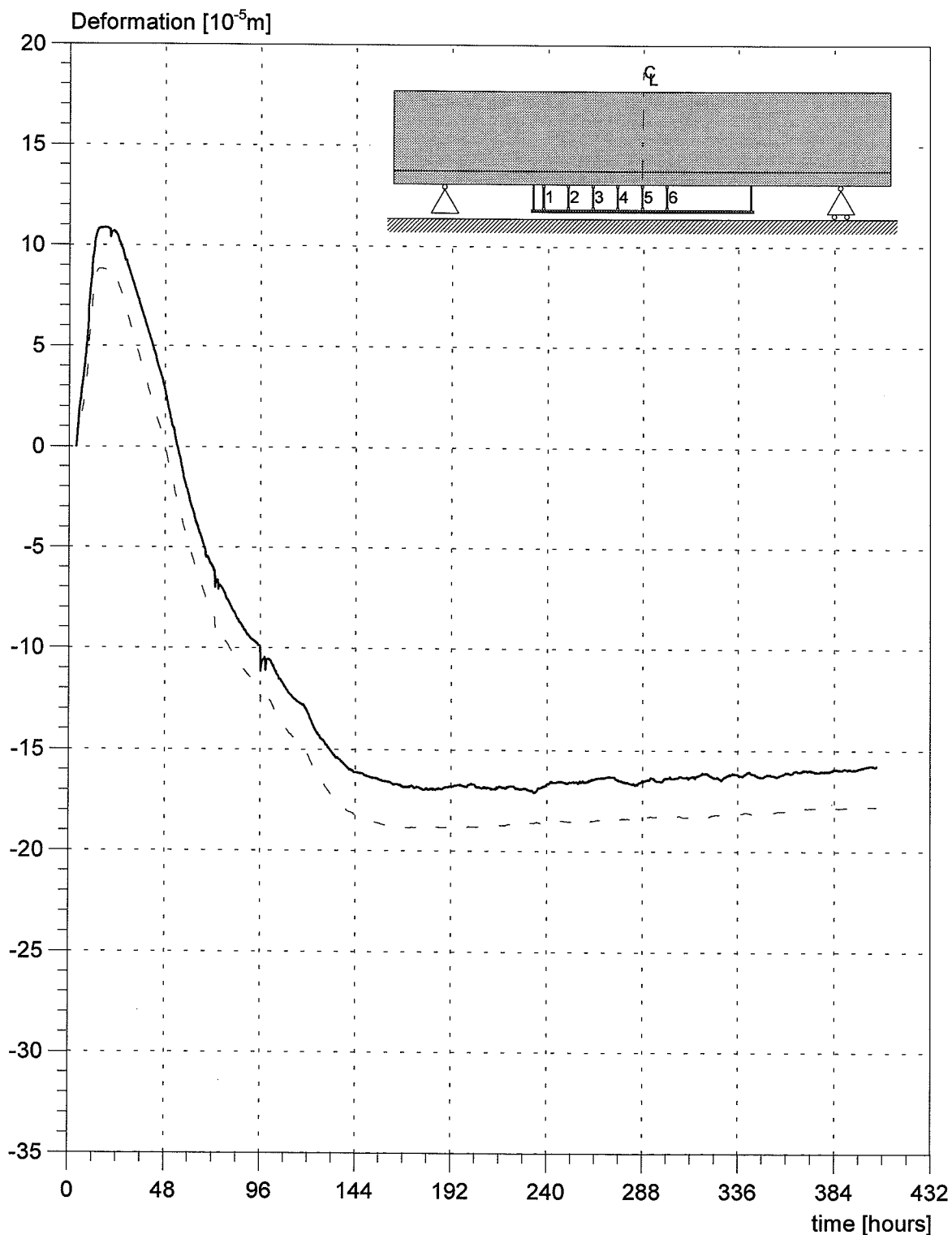
DTI Building Technology  
Gregersensvej, 2630 Taastrup

Vertical deformation  
transducer no. 2

Client: HETEK 3 + 4  
Name: Stage 7

Ref.: 53459  
Date: 02/25/97

Init.: HSP/ESP



t = 0 at time of mixing  
Start of measurements at t=3.499 h

— temp. compensated  
- - measured

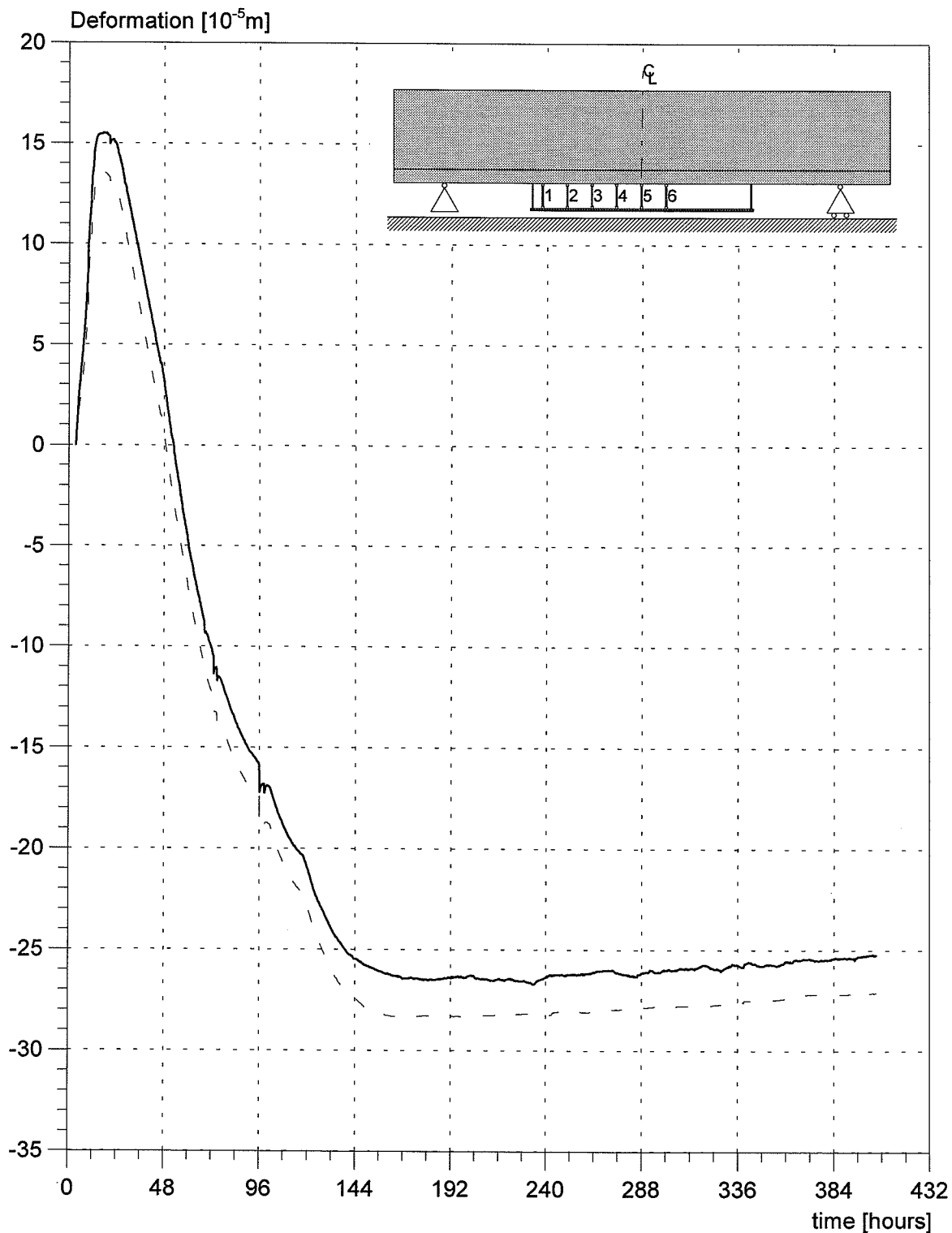
DTI Building Technology  
Gregersensvej, 2630 Taastrup

Vertical deformation  
transducer no. 3

Client: HETEK 3 + 4  
Name: Stage 7

Ref.: 53459  
Date: 02/25/97

Init.: HSP/ESP



t = 0 at time of mixing  
Start of measurings at t=3.499 h

— temp. compensated  
- - measured

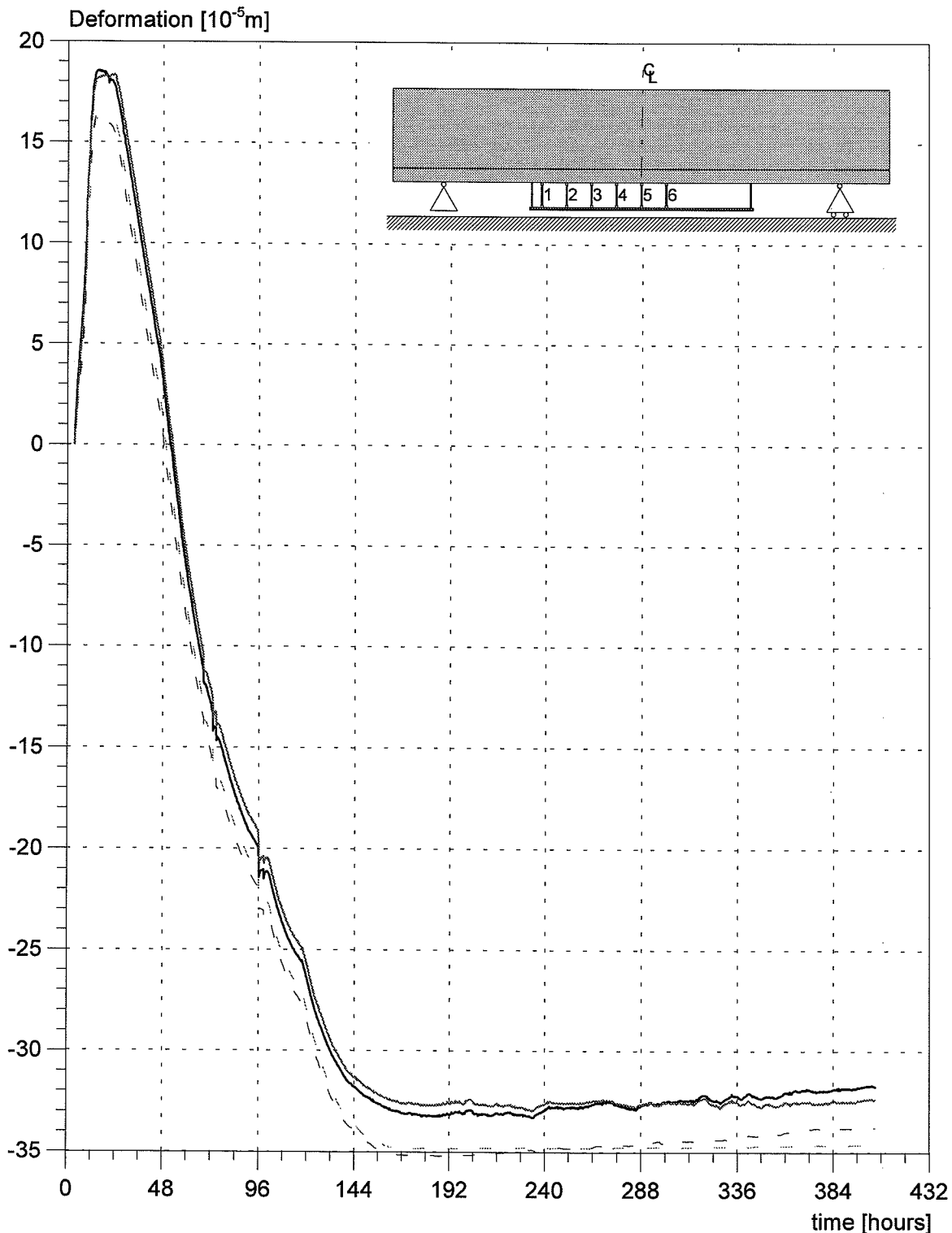
DTI Building Technology  
 Gregersensvej, 2630 Taastrup

Vertical deformation  
 transducer no. 4 & 6

Client: HETEK 3 + 4  
 Name: Stage 7

Ref.: 53459  
 Date: 02/25/97

Init.: HSP/ESP



t = 0 at time of mixing  
 Start of measurings at t=3.499 h

- temp. compensated - no. 4
- temp. compensated - no. 6
- - measured - no. 4
- - measured - no. 6

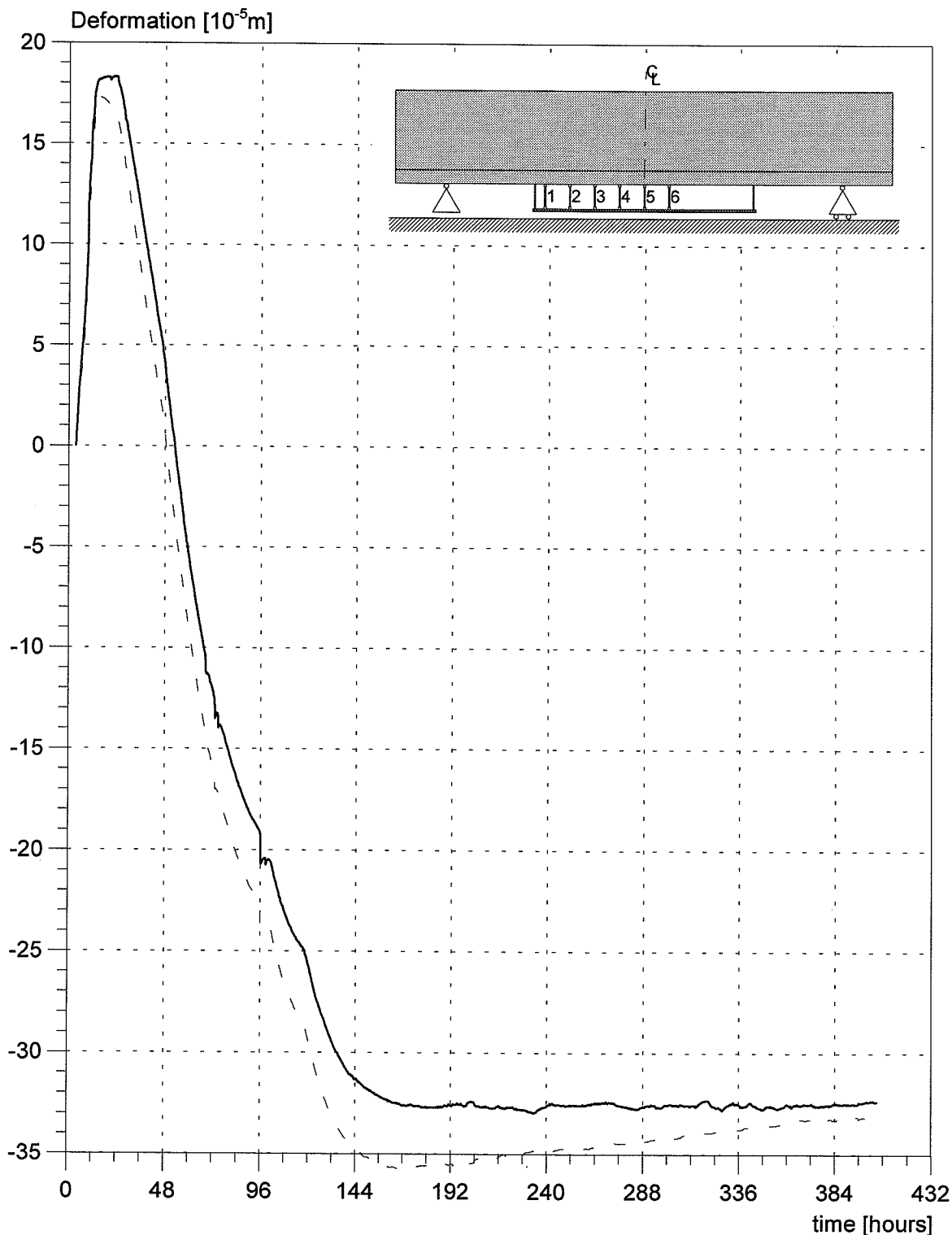
DTI Building Technology  
 Gregersensvej, 2630 Taastrup

Vertical deformation  
 transducer no. 5

Client: HETEK 3 + 4  
 Name: Stage 7

Ref.: 53459  
 Date: 02/25/97

Init.: HSP/ESP



t = 0 at time of mixing  
 Start of measurings at t=3.499 h

— temp. compensated  
 - - - measured



## **APPENDIX J**

### **Measured deformations relative to the fixed plane**

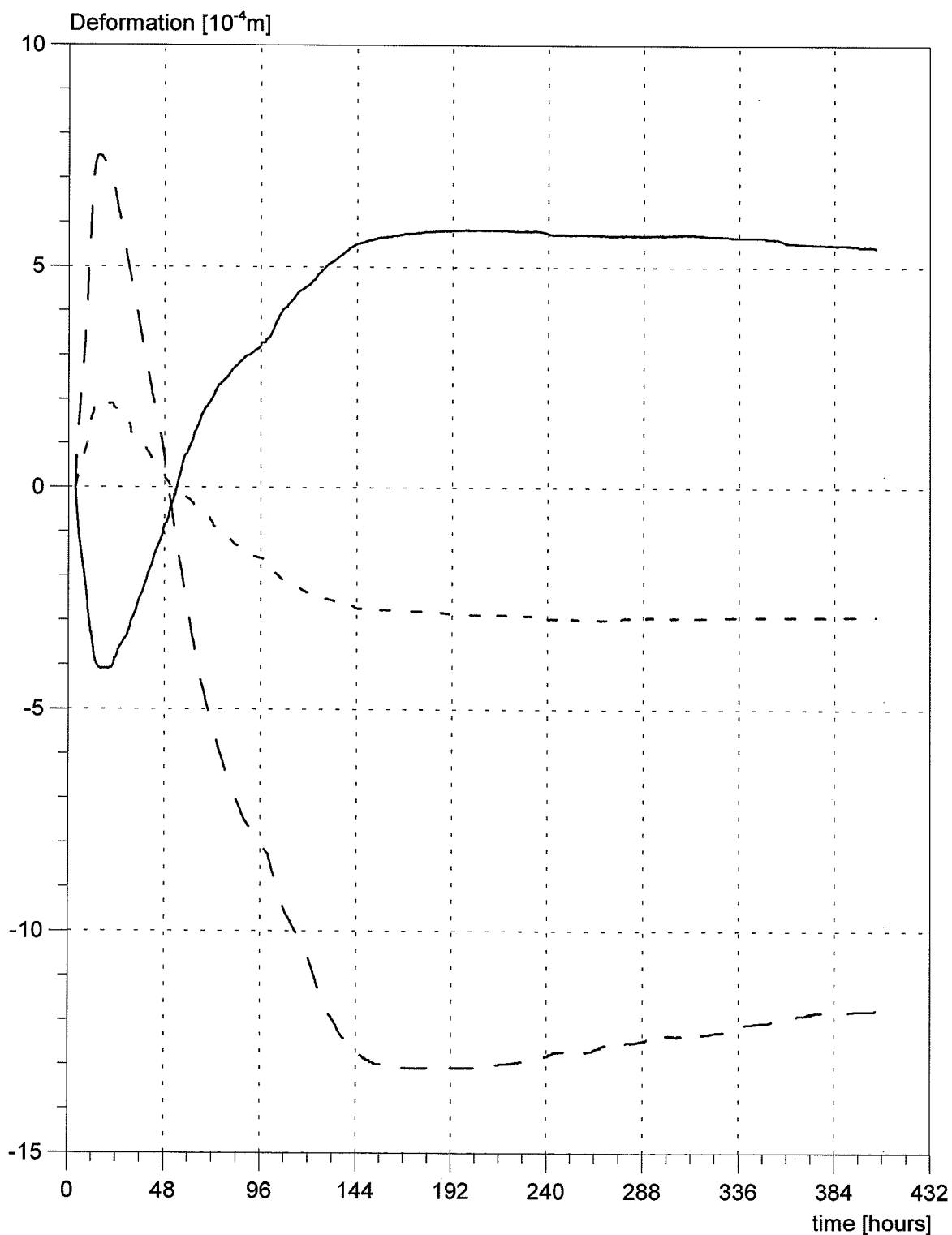
DTI Building Technology  
Gregersensvej, 2630 Taastrup

Vertical deformation  
transducer no. A, B & C

Client: HETEK 3 + 4  
Name: Stage 7

Ref.: 53459  
Date: 02/25/97

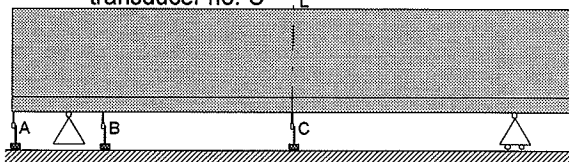
Init.: HSP/ESP



$t = 0$  at time of mixing  
Start of measurements at  $t = 3.499$  h

NB! Not compensated for temperature deformations  
in transducers.

— transducer no. A  
- - transducer no. B  
- · transducer no. C



## **APPENDIX K**

### **Measured longitudinal deformations**

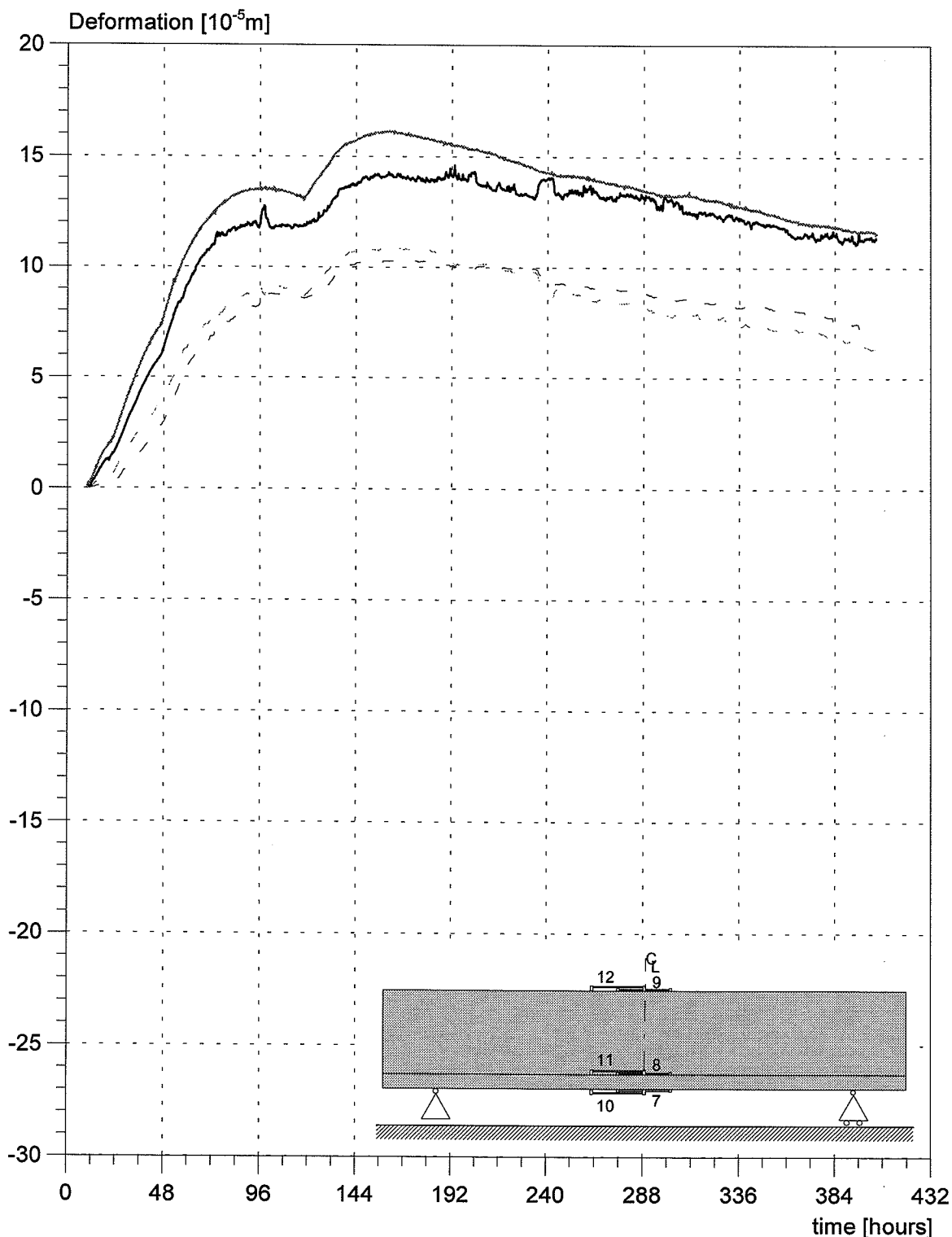
DTI Building Technology  
 Gregersensvej, 2630 Taastrup

Horizontal deformation  
 transducer no. 7 & 10

Client: HETEK 3 + 4  
 Name: Stage 7

Ref.: 53459  
 Date: 02/25/97

Init.: HSP/ESP



t = 0 at time of mixing  
 Start of measurements at t = 9.7 h  
 The deformation is measured over a length of 1 m.

- temp. compensated - no. 7
- temp. compensated - no. 10
- - measured - no. 7
- · · measured - no. 10

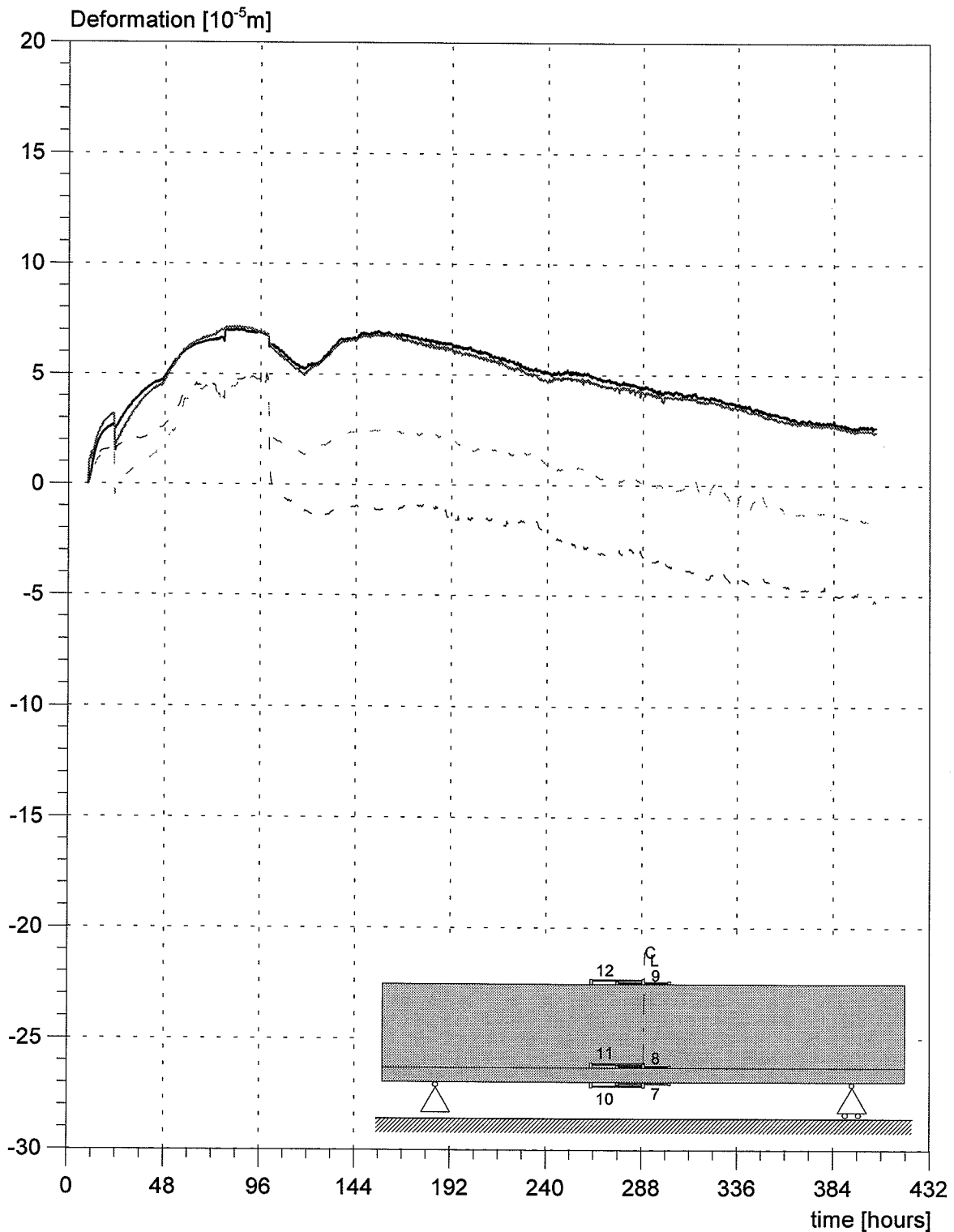
DTI Building Technology  
Gregersensvej, 2630 Taastrup

Horizontal deformation  
transducer no.8 & 11

Client: HETEK 3 + 4  
Name: Stage 7

Ref.: 53459  
Date: 02/25/97

Init.: HSP/ESP



t = 0 at time of mixing  
Start of measurings at t=9.7 h  
The deformation is measured over a length of 1 m.

— temp. compensated - no. 8  
— temp. compensated - no. 11  
- - measured - no. 8  
- - measured - no. 11

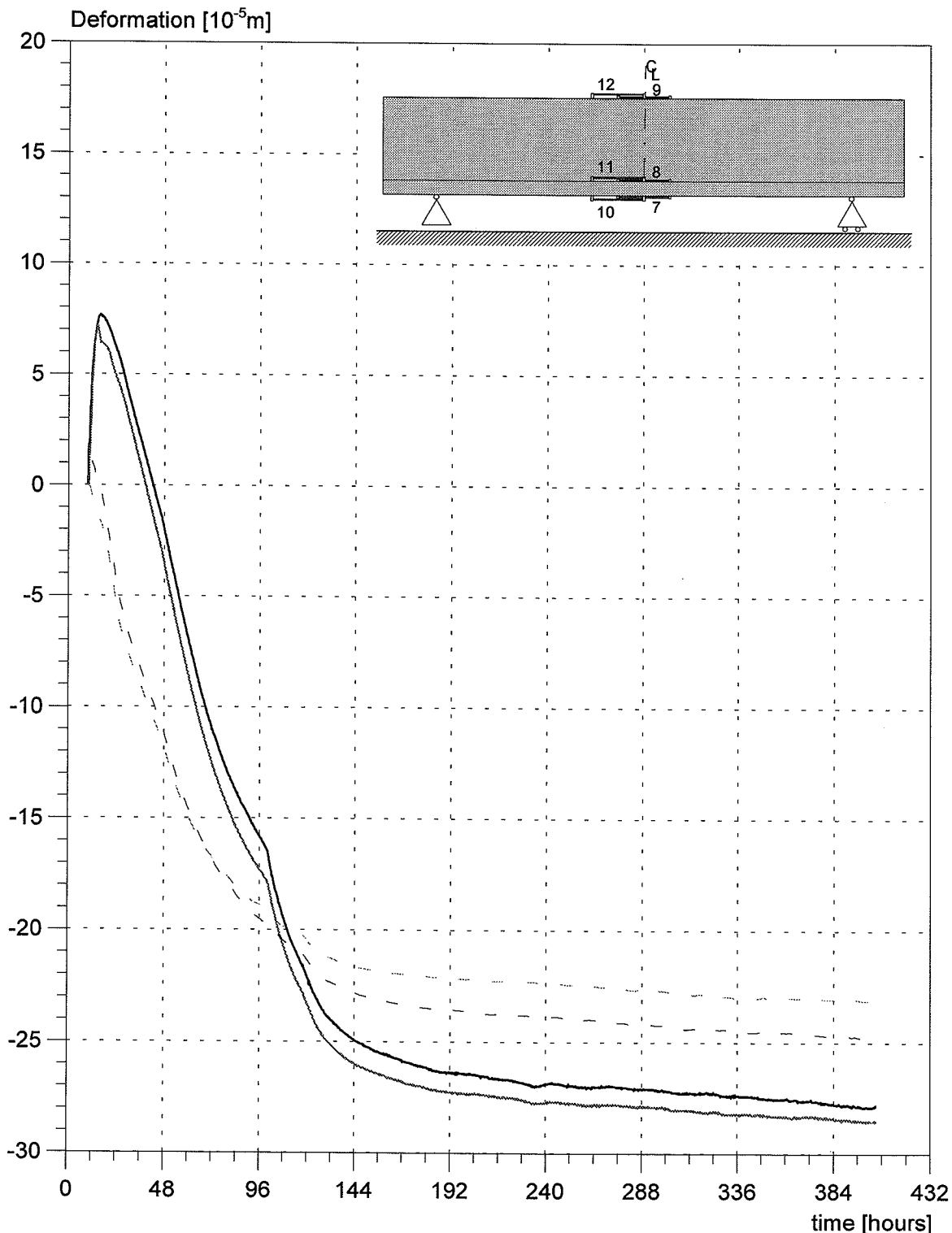
DTI Building Technology  
 Gregersensvej, 2630 Taastrup

Horizontal deformation  
 transducer no. 9 & 12

Client: HETEK 3 + 4  
 Name: Stage 7

Ref.: 53459  
 Date: 02/25/97

Init.: HSP/ESP



t = 0 at time of mixing  
 Start of measurements at t=9.7 h  
 The deformation is measured over a length of 1 m.

- temp. compensated - no. 9
- temp. compensated - no. 12
- - - measured - no. 9
- - - measured - no. 12

## **APPENDIX L**

### **Measured acoustic emission**

## Appendix L Measured acoustic emission

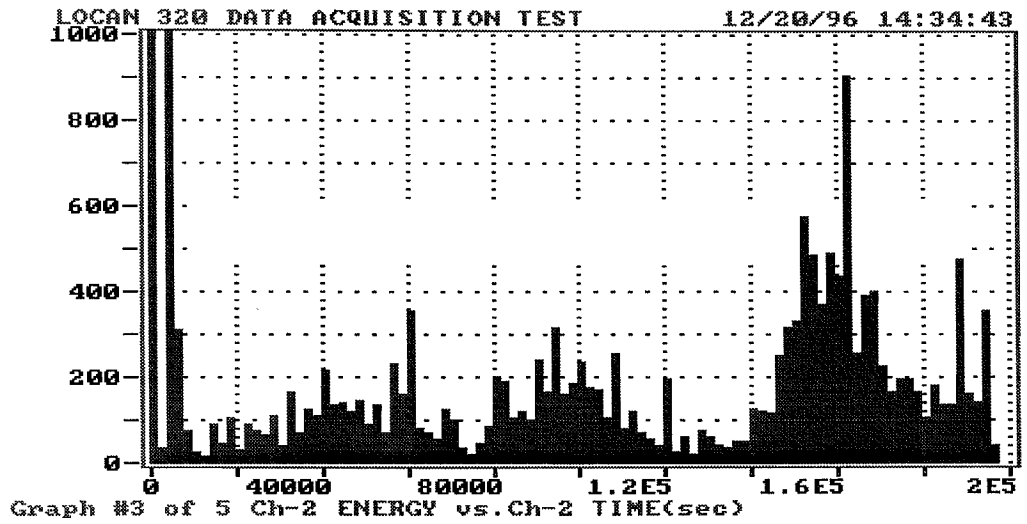


Figure L.1- Energy as a function of time, measured by acoustic emission. The starting-time of the measurements corresponds to 98.3 hours after mixing.

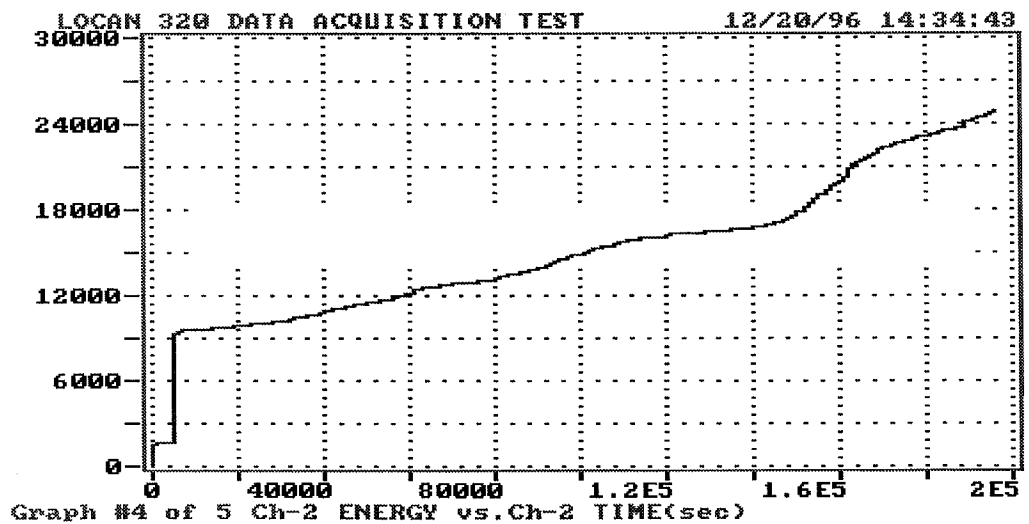


Figure L.2 Cumulative energy as a function of time, measured by acoustic emission. The starting-time of the measurements corresponds to 98.3 hours after mixing.



## **APPENDIX M**

### **Assumptions underlying the calculations**

Client: HETEK

Ref. nr.:

Project: fase7-2c

Date: 04/14/97

Name: phase 7

Initials :

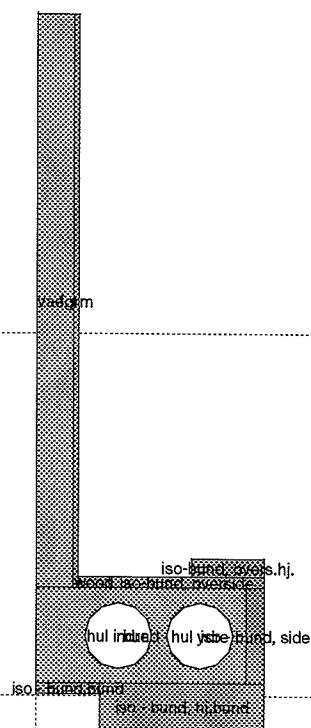
Id. nr. : VE-AA1467

Time: 08:54

## Volumes

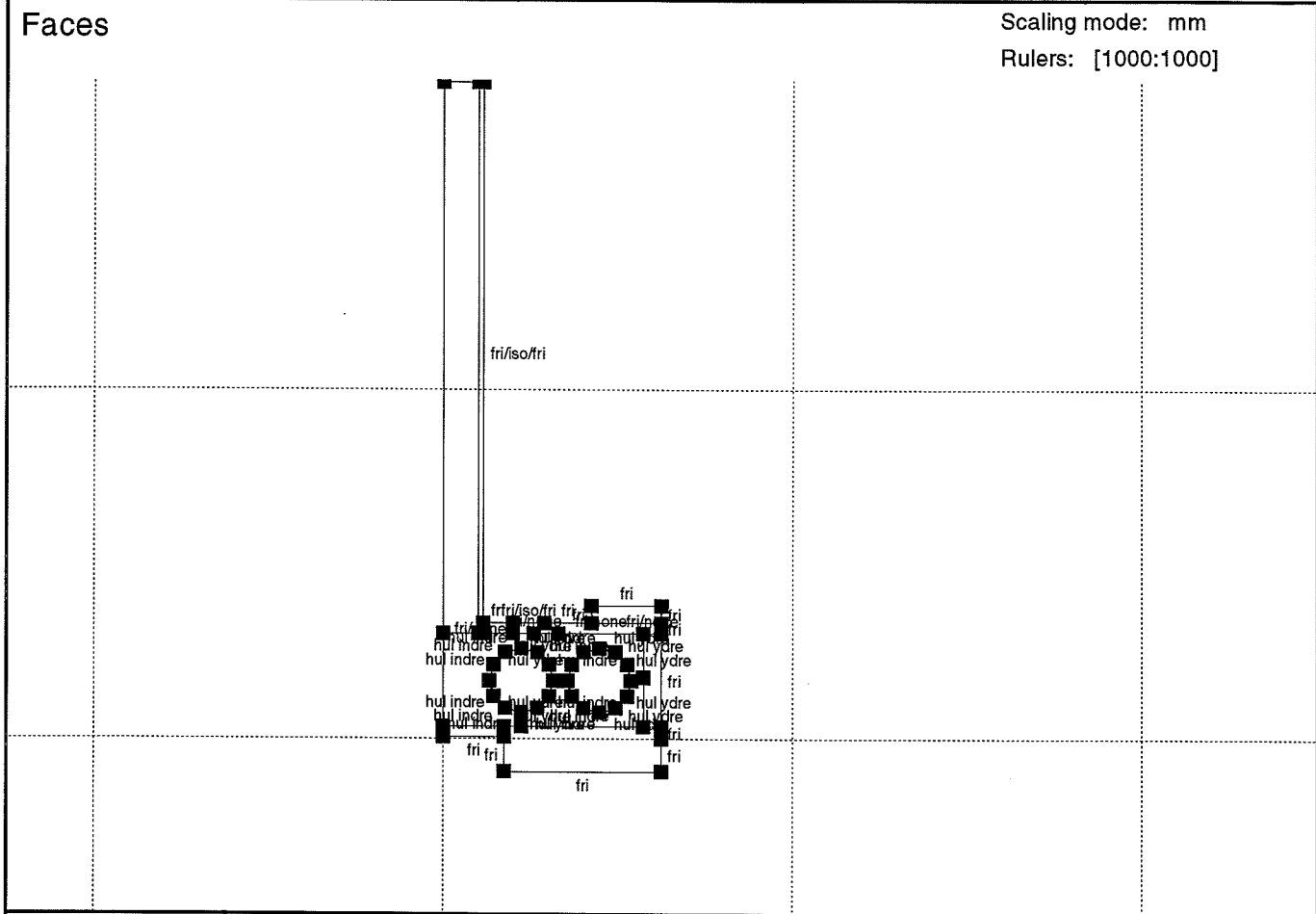
Scaling mode: mm

Rulers: [1000:1000]



Volume	Size [ mm ]	Material type [ - ]	Material name [ - ]	Thickness [ m ]	Start time [ h ]	Temp. [ °C ]
vaeg	100 by 1580	Concrete	Hetek fase1 ny kryb	1000.	0.	18.
hul indre	183 by 183	(none)	-	-	-	-
hul ydre	183 by 183	(none)	-	-	-	-
bund	575 by 265	Concrete	bund E = 45000	1000.	0.	18.
iso - bund,bund	175 by 30	Material	Poly-bund	1000.	0.	18.
iso - bund, side	50 by 265	Material	Poly-bund	1000.	0.	18.
iso - bund, hj.bund	450 by 130	Material	Poly-bund	1000.	0.	18.
form	15 by 1580	Material	formx	1000.	0.	18.
wood	85 by 30	Material	formx	1000.	0.	18.
iso-bund, overs.hj.	200 by 50	Material	Poly-bund	1000.	23.	20.2
iso-bund, overside	425 by 30	Material	Poly-bund	1000.	23.	20.2

Client: HETEK	Ref. nr.:	Project: fase7-2c	Date: 04/14/97
Name: phase 7	Initials :	Id. nr. : VE-AA1467	Time: 08:58



Boundary condition	Functions				
	Temperature	Wind velocity	Shield definition	Coef. of transm.	Flux
fri	temp20	vind1	fri	fri	-
fri/none	temp20	-	-	fri/none	-
fri/iso/fri	temp20	-	-	fri/iso/fri	-
hul indre	hul indre	vind5	fri	hul indre	-
hul ydre	hul ydre	vind5	fri	hul ydre	-
top	temp20	-	-	top	-

DTI Building Technology Gregersensvej, DK 2630 Taastrup	<b>CALCULATION BASIS</b> Documentation sheet
--	---

Client: HETEK Name: phase 7	Ref. nr.: Initials :	Project: fase7-2c Id. nr. : VE-AA1467	Date: 04/14/97 Time: 08:58
--------------------------------	-------------------------	--	-------------------------------

**Functions**

Name	Type	Description	Unit	Function table Time [h] / Value
temp20	Temperature	Linear curve	[ °C ]	0. / 18. - 1.67 / 18. - 1.68 / 14. - 2.17 / 16. - 2.67 / 15. - 3.17 / 19. - 3.67 / 19.5 - 4.17 / 19.6 - 5.17 / 20. - 6.17 / 20.4 - 7.17 / 20.7 - 8.17 / 20.9 - 9.17 / 21.3 - 10.17 / 21.6 - 12.17 / 21.3 - 13.67 / 21.3 - 13.92 / 20.7 - 20.17 / 20.8 - 53.17 / 20.5 - 100.17 / 20.8 - 125.17 / 20.4 - 150.17 / 20.6 - 175.17 / 20.3 - 200.17 / 20.3 - 225.17 / 20. - 235.17 / 19.6 - 240.17 / 20.7 - 250.17 / 20. - 265.17 / 20.4 - 285.17 / 20.2 - 1000. / 20.2
hul ydre	Temperature	Linear curve	[ °C ]	0. / 18. - 1.67 / 18. - 4.17 / 19. - 22.57 / 21.6 - 23.17 / 22.5 - 24.17 / 23.4 - 25.17 / 24. - 28.17 / 25. - 30.17 / 25.8 - 34.17 / 27. - 40.17 / 28.1 - 46.17 / 29. - 48.17 / 29.7 - 52.17 / 31. - 58.17 / 32.5 - 64.17 / 33.6 - 72.17 / 34.5 - 80.17 / 35.2 - 90.17 / 35.7 - 100.17 / 35.9 - 106.17 / 36. - 118.17 / 36. - 118.67 / 37. - 120.17 / 37.7 - 124.17 / 38.6 - 130.17 / 39.4 - 138.17 / 40.2 - 150.17 / 40.7 - 170.17 / 41. - 200.17 / 41. - 1000. / 41.

DTI Building Technology Gregersensvej, DK 2630 Taastrup		CALCULATION BASIS Documentation sheet		
Client: HETEK Name: phase 7		Ref. nr.: Initials :	Project: fase7-2c Id. nr. : VE-AA1467	Date: 04/14/97 Time: 08:58
Functions				
Name	Type	Description	Unit	Function table Time [h] / Value
hul indre	Temperature	Linear curve	[ °C ]	0. / 18. - 1.67 / 18. - 4.17 / 19. - 22.57 / 21.6 - 24.17 / 22.6 - 25.17 / 23. - 30.17 / 24.5 - 34.17 / 25.6 - 40.17 / 26.7 - 46.17 / 27.8 - 48.17 / 30. - 52.17 / 31. - 58.17 / 32. - 64.17 / 33.1 - 72.17 / 34. - 80.17 / 34.7 - 90.17 / 35.2 - 100.17 / 35.5 - 106.17 / 35.5 - 118.17 / 35.4 - 120.17 / 36. - 124.17 / 36.7 - 130.17 / 37.4 - 138.17 / 38.2 - 150.17 / 38.7 - 170.17 / 39.2 - 200.17 / 39.2 - 1000. / 39.2
vind1	Wind velocity	Piecewise	[ m/s ]	0. / 1. - 1000. / 1.
vind5	Wind velocity	Piecewise	[ m/s ]	0. / 5. - 1000. / 5.
fri	Transm. coef.	Piecewise	[ kJ/m <sup>2</sup> /h/°C ]	0. / 34. - 1000. / 34.
fri/none	Transm. coef.	Piecewise	[ kJ/m <sup>2</sup> /h/°C ]	0. / 34. - 23. / 0. - 1000. / 34.
fri/iso/fri	Transm. coef.	Piecewise	[ kJ/m <sup>2</sup> /h/°C ]	0. / 22.8 - 10.67 / 15. - 14. / 25. - 16. / 30. - 18. / 35. - 26. / 30. - 30. / 20. - 40. / 15. - 54. / 10. - 70. / 5. - 100.17 / 50. - 1000. / 50.
hul indre	Transm. coef.	Piecewise	[ kJ/m <sup>2</sup> /h/°C ]	0. / 90. - 1000. / 90.
hul ydre	Transm. coef.	Piecewise	[ kJ/m <sup>2</sup> /h/°C ]	0. / 90. - 1000. / 90.
top	Transm. coef.	Piecewise	[ kJ/m <sup>2</sup> /h/°C ]	0. / 1.5 - 10. / 10. - 15. / 30. - 17. / 15. - 20. / 5. - 25. / 2. - 30. / 0.8 - 100.17 / 1.5 - 1000. / 1.5

DTI Building Technology Gregersensvej, DK 2630 Taastrup	CALCULATION BASIS Documentation sheet		
--	--	--	--

Client: HETEK	Ref. nr.:	Project: fase7-2c	Date: 04/14/97
Name: phase 7	Initials :	Id. nr. : VE-AA1467	Time: 09:03

**Calculation parameters**

Thermal analysis	Transient	Circles	
Stress analysis	Based on thermal results	No. of faces	12
Dimensions			
2½-Dimensional	-	Self weight	
	-	Direction X	-
	No rotation around y-axis	Direction Y	-
Time specifications		Mesh, node generation	
Total process time	408.	Percentage of the largest extend	
Time step, desired	2.	Min. distance to border	0.10
Time step, factor	0.6	Density, internal nodes	3.00
		Density, border nodes	3.00
Nonlinear calculations		Density, around c-pipes	1.50
Convergence criteria	1.000e-03	Radius around c-pipes	5.00

<b>DTI Building Technology</b> Gregersensvej, DK 2630 Taastrup	<b>CALCULATION BASIS</b> Documentation sheet
---	---

Client: HETEK	Ref. nr.:	Project: fase7-2c	Date: 04/14/97
Name: phase 7	Initials :	Id. nr. : VE-AA1467	Time: 08:57

<b>Material database</b>	<b>Poly-bund</b>
--------------------------	------------------

**MATERIAL PROPERTIES**

Density	[ kg/m <sup>3</sup> ]	30.
Specific heat	[ kJ/kg/°C ]	5.
Thermal conductivity	[ kJ/m/h/°C ]	1.
Thermal expansion	[ 1/°C ]	0.
E-modulus	[ MPa ]	10.
Poisson ratio	[ - ]	0.
Comp. strength	[ MPa ]	1000.
Tensile strength	[ MPa ]	1000.

Client: HETEK

Ref. nr.:

Project: fase7-2c

Date: 04/14/97

Name: phase 7

Initials :

Id. nr. : VE-AA1467

Time: 08:57

## Material database

formx

## MATERIAL PROPERTIES

Density	[ kg/m <sup>3</sup> ]	700.
Specific heat	[ kJ/kg/°C ]	3.
Thermal conductivity	[ kJ/m/h/°C ]	0.25
Thermal expansion	[ 1/°C ]	0.
E-modulus	[ MPa ]	10.
Poisson ratio	[ - ]	0.
Comp. strength	[ MPa ]	1000.
Tensile strength	[ MPa ]	1000.